

UNCLASSIFIED

AD 405 680

DEFENSE DOCUMENTATION CENTER

FOR

SCIENTIFIC AND TECHNICAL INFORMATION

CAMERON STATION, ALEXANDRIA, VIRGINIA



UNCLASSIFIED

NOTICE: When government or other drawings, specifications or other data are used for any purpose other than in connection with a definitely related government procurement operation, the U. S. Government thereby incurs no responsibility, nor any obligation whatsoever; and the fact that the Government may have formulated, furnished, or in any way supplied the said drawings, specifications, or other data is not to be regarded by implication or otherwise as in any manner licensing the holder or any other person or corporation, or conveying any rights or permission to manufacture, use or sell any patented invention that may in any way be related thereto.

63-3-5

405689

ASD-TR-61-713
Part II

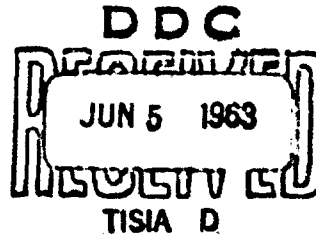
RESEARCH ON THE BASIC NATURE OF
STRESS CORROSION FOR VARIOUS STRUCTURAL ALLOYS AT
ROOM AND ELEVATED TEMPERATURES

TECHNICAL DOCUMENTARY REPORT NO. ASD-TR-61-713, PT. II
February 1963

405680

Directorate of Materials and Processes
Aeronautical Systems Division
Air Force Systems Command
Wright-Patterson Air Force Base, Ohio

Project 7351, Task 735106



(Prepared under Contract No. AF 33(616)-7612
by the Armour Research Foundation, Chicago, Illinois;
Frank A. Crossley, author.)

NOTICES

When Government drawings, specifications, or other data are used for any purpose other than in connection with a definitely related Government procurement operation, the United States Government thereby incurs no responsibility nor any obligation whatsoever; and the fact that the Government may have formulated, furnished, or in any way supplied the said drawings, specifications, or other data, is not to be regarded by implication or otherwise as in any manner licensing the holder or any other person or corporation, or conveying any rights or permission to manufacture, use, or sell any patented invention that may in any way be related thereto.

- - - - -

Qualified requesters may obtain copies of this report from the ASTIA Document Service Center, Arlington Hall Station, Arlington 12, Virginia.

- - - - -

This report has been released to the Office of Technical Services, Department of Commerce, Washington 25, D.C., for sale to the general public.

- - - - -

Copies of ASD Technical Reports and Technical Notes should not be returned to the Aeronautical Systems Division unless return is required by security considerations, contractual obligations, or notice on a specific document.

FOREWORD

This report was prepared by Armour Research Foundation under USAF Contract No. AF 33(616)-7612. The contract was initiated under Project No. 1(8-7351), "Metallic Materials" and Task No. 735106, "Behavior of Metals." The work was administered under the direction of Directorate of Materials and Processes, Deputy for Technology, Aeronautical Systems Division, Air Force Systems Command, with Mr. R. T. Ault acting as project engineer.

The contract period was from 15 December 1961 to 16 February 1963.

Armour Research Foundation personnel who made major contributions to the program were: F. A. Crossley, project leader; T. Niemczyk and B. J. Stang, project technicians; J. E. Lenke and H. Sheriff, technicians, metallurgical services; and J. R. Dvorak, H. Konjevich and R. F. Dragen, metallographers. The data reported herein are recorded in ARF Logbooks Nos. C-12051, C-12432, C-12433, and C-12920, assigned to Project No. ARF B206. This report is identified internally as ARF-B206-12.

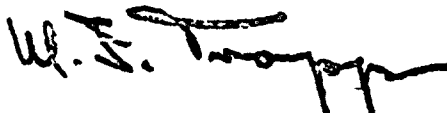
ABSTRACT

The objectives of this program were: (1) to study the effect of microstructure on susceptibility to stress-corrosion cracking in the short-transverse direction of 7075-T6 aluminum alloy; and (2) to study the kinetics of stress-corrosion cracking at elevated temperature of candidate materials for structural applications in the trisonic transport in the presence of sea salt.

It was hypothesized that the poor resistance to stress corrosion of high-strength, wrought aluminum alloys was due to the layered type microstructure characteristic of these materials. Phases which are out of solid solution in the original as-cast structure tend to be concentrated in the grain boundaries. During working, the original grains are flattened out into plates and, therefore, the second phase particles are distributed in layers. During the solution heat treatment the recrystallized grains grow until the growth is inhibited by these second-phase particles. As a consequence, the wrought, heat-treated product has planes of weakness parallel to the major direction of working. Commercial 7075-T6 and materials of the same composition prepared in the laboratory in the form of 1 in. plate were compared as to susceptibility to stress corrosion in the short-transverse direction. In these materials short life was associated with the layered type of grain structure characteristic of commercial material, and long life was associated with irregular or equiaxed grain structures. The experimental results gave good support to the hypothesis.

Apparatus was set up to measure elevated-temperature crack growth kinetics by monitoring resistance with a precision Kelvin bridge. Preliminary trials with Ti-8Al-1Mo-1V alloy showed promise. Exposures of AM 350 CR 20% and PH 15-7Mo RH 1050 under stress at temperatures from 650° to 800°F gave no indications that these materials are susceptible to chloride salt stress corrosion.

This technical documentary report has been reviewed and is approved.



W. J. TRAPP
Chief, Strength and Dynamics Branch
Metals and Ceramics Laboratory
Directorate of Materials and Processes

TABLE OF CONTENTS

	Page
I. PART I - STRESS CORROSION OF 7075-T6	1
A. Introduction	1
B. Experimental Methods.	1
1. Preparation of Test Materials	1
2. Stress-Corrosion Tests.	3
3. Tensile Tests	3
4. Microprobe Analysis.	3
5. Residual Stress Determination	4
C. Results and Discussion	4
1. Microstructures	4
2. Microprobe Analysis of Second-Phase Particles in 7075-T6	5
3. Tensile Test Results.	6
4. Residual Stress	6
5. Stress-Corrosion Test Results	7
D. Summary and Conclusions	8
II. PART II - STRESS CORROSION OF SST CANDIDATE MATERIALS	10
A. Introduction	10
B. Experimental Methods.	10
C. Results and Discussion	11
REFERENCES	14

LIST OF ILLUSTRATIONS

Figure		Page
1	Shear Inducer	27
2	Stress Corrosion Test Specimen for Evaluation of Susceptibility in the Short-Transverse Direction of Plate	28
3	Stress-Corrosion Test Units and Detail of Specimen Loading Arrangement	29
4	Tensile Test Specimen for 7075-T6 Materials	30
5	Macrographs of cast ingots of 7075 alloy; Left--high-purity, fine grain size; Center--high purity, coarse grain size; and Right--remelted commercial stock, fine grain size.	31
6	Microstructures of 7075-T6 commercial plate 1-in. thick	32
7	Microstructures showing distribution of second-phase particles in 7075-T6 commercial plate 1-inch thick .	33
8	Microstructures of 7075-T6 commercial purity plate 1-inch thick, remelted and grain refined	34
9	Microstructures showing distribution of second-phase particles in 7075-T6 commercial purity plate 1-inch thick, grain refined	35
10	Microstructures of 7075-T6 high-purity plate 1-inch thick, coarse grain size	36
11	Microstructures showing distribution of second-phase particles in 7075-T6 high-purity plate 1-inch thick, coarse grain size.	37
12	Microstructures of 7075-T6 high-purity plate 1-inch thick, fine grain size	38
13	Microstructures showing distribution of second-phase particles 7075-T6 high-purity plate 1-inch thick, fine grain size	39
14	Areas on plane parallel to the rolling plane examined with the microprobe analyser. Commercial 7075-T6 plate 1-inch thick.	40
15	Electron image of region I. Bright areas represent higher average atomic number than that of the matrix.	41
16	Mg K α image of region I shows dark particles to be rich in magnesium	41
17	Cu K α image of zone A of region I shows gray particles to be copper-rich	41

LIST OF ILLUSTRATIONS (Cont.)

Figure		Page
18	Electron image of region II	42
19	Al K _a image of zone B in region II shows dark particles to be aluminum-poor.	42
20	One end of each of the fractured tensile test specimens of 7075-T6 materials. From left to right: (1) commercial (2) commercial, grain refined; (3) high-purity, coarse grain size; and (4) high-purity, fine grain size.	43
21	Stress Corrosion Results for 7075-T6 Materials Immersed in Daily Changed Bath of NaCl-H ₂ O ₂ -Aerosol Solution	44
22	Stress Corrosion Results for 7075-T6 Materials Immersed in Daily Changed Bath of NaCl-H ₂ C ₂ Solutions.	45
23	Stress Corrosion Results for 7075-T6 Materials Immersed in Daily Changed Bath of CrO ₃ Solution . .	46
24	Smooth and Notched Specimens	47
25	Change in Resistance with Crack Length for Ti-8Al-1Mo-1V Specimens.	48

LIST OF TABLES

Table	Page
1 Materials for 7075 Aluminum Alloy Melts	15
2 Chemistry of 7075 Materials	16
3 Tensile Test Properties of 7075-T6 Materials	17
4 Residual Stress of 7075-T6 Materials	18
5 Stress-Corrosion Results for 7075-T6 Materials in NaCl-H ₂ O ₂ -Aerosol Solution	19
6 Stress-Corrosion Results for 7075-T6 Materials in NaCl-H ₂ O ₂ Solution	20
7 Stress Corrosion Results for 7075-T6 Materials in Chromate Solutions	21
8 Summary of Surface and Metallographic Observations on Exposed Stress-Corrosion Specimens of 7075-T6 Materials	22
9 Chemistry of Trisonic Transport Candidate Materials .	24
10 Tensile Test Properties of SST Candidate Materials .	25
11 Stress-Corrosion Susceptibility Survey of SST Candidate Materials	26

I. PART I - STRESS CORROSION OF 7075-T6

A. Introduction

High-strength, wrought aluminum-base alloys are considerably less resistant to stress-corrosion cracking in the short-transverse direction than in the long-transverse or the longitudinal direction. When the microstructure of such a material is examined, it is at once apparent that the grains are elongated in the direction of rolling or working. It appears that at periodic intervals a barrier to grain growth exists. The microstructure suggests that these barriers may be traces of the original as-cast grain boundaries. The stress-corrosion behavior indicates that these regions represent planes of weakness. In a test of the short-transverse direction, the stress direction is perpendicular to the plane of these barriers to grain growth, and the crack propagates intergranularly along these planes. The as-cast grain boundary is the likely site of (a) whatever insoluble particles are present in the melt, (b) precipitates of impurities having low solubilities, and (c) precipitates from the supersaturated liquid that is last to solidify. Subsequent processing would have no effect on the insoluble phases and, very likely, would not entirely eliminate the other precipitated phases. Judging from the microstructures, processing acts to spread out the second-phase particles and produces the layered structure observed.

Assuming that the above hypothesis explains the observed directionality in stress-corrosion sensitivity, a program was undertaken to study the effect of eliminating or at least greatly minimizing the layer structure by means of a casting technique. Four materials of the 7075 alloy in the form of one-inch plate were evaluated; they were:

- (1) normal commercial material,
- (2) commercial material remelted, fluxed to remove insoluble particles, and cast under conditions to produce a fine grain size,
- (3) high-purity melt cast under conditions to produce a coarse grain size, and
- (4) high-purity melt cast under conditions to produce a fine grain size.

Evaluation consisted of stress-corrosion testing in aqueous solutions, metallographic examination, electron beam microprobe analysis of phases present in normal commercial material, and determination of the residual stress in the plane perpendicular to the rolling direction.

B. Experimental Methods

I. Preparation of Test Materials

Originally it was sought to make the fine-grained ingots exceptionally fine grained by combining two grain-refining techniques: inoculation by

means of titanium addition (1), and application of viscous shear, i.e., rotational acceleration (2). The apparatus depicted in Fig. 1 was constructed for imparting viscous shear during solidification to 30 pounds of metal. This was accomplished by accelerating rapidly to a high rotational speed and decelerating rapidly by applying a brake. When the brake was released, acceleration occurred again. The period of the acceleration-deceleration cycle was controlled by a timer mechanism. While this apparatus was being completed, several ingots of 7075 alloy were prepared in a consumable electrode arc-melting furnace with magnetic stirring applied to give grain refinement (3).

Difficulties were encountered in preparing fine-grained ingots of 7075 alloy both by means of consumable arc melting with magnetic stirring and by mechanical stirring of cast metal during solidification. In the former case the expected deep pool of molten metal was not formed; and the metal appeared to solidify in layers about $1/16$ - $1/8$ inch thick, often separated near the outside by cold shuts. The ingot was fine-grained but not to the extent expected on the basis of earlier work. In the latter case the grain structure was not sufficiently refined to suit the needs of this program. Several factors may underlie these observed differences in results. One factor which appears to be of major importance is the liquidus-solidus temperature differential.

Prior experience in the application of viscous shear has been with relatively pure metals--that is, 1100 aluminum alloy (99 +% purity) and grade A nickel (99.4% Ni + Co). In the case of 1100 aluminum alloy and grade A nickel this temperature differential is 25° and 20° F, respectively, while the differential of 7075 is 280° F (4). This means that in the relatively pure metals there is a fairly well defined solid/liquid interface with little if any nucleation occurring much in advance of it. On the other hand, the solid/liquid interface of the 7075 alloy would be ill-defined and would be very deep; also nucleation would show significant occurrence in advance of the interface zone.

The question to be resolved in this program was, Can as-cast grain size influence resistance to stress-corrosion susceptibility through its influence on the distribution of insoluble or precipitate phases? This purpose could be served by using conventional techniques to produce ingots having a significant difference in grain size. Therefore, to produce materials for evaluation without further delay, a coarse-grained ingot cast from high-purity materials and fine-grained ingots cast from commercial 7075 plate and from virgin, high-purity materials were made. The nominal composition of 7075 alloy is: 5.5 Zn, 2.5 Mg, 1.5 Cu, 0.3 Mn, and 0.3 Cr. (All compositions in this report are given in weight per cent unless otherwise noted.) The purity, source, and form of the metals used for the high-purity melts are reported in Table 1. The fine-grained ingots were cast at 1300° F into 1-inch thick walled, cylindrical steel molds and inoculated with additions of 0.36% titanium added as Ti-44% Al master alloy. The coarse-grained ingot was cast at 1500° F into a sand mold. The ingots were approximately 4 inches in diameter by 5 inches in height after removing the riser.

The ingots were turned down $1/8$ inch on the radius, then soaked at 885° F for 24 hours, and transferred to a furnace at 825° F preparatory to initial breakdown by press forging. The ingots were initially upset by

press-forging and then side-forged between 700° and 825°F to 1 1/2-inch thick plate. The plates were rolled to 1 1/16 inches at 700°F in 0.050-inch passes. The rolled plates were then heat-treated as follows: 860°F-1 hr, cold-water quenched, aged 250°F-24 hr, air cooled.

Results of chemical analyses on the 7075 materials together with nominal compositions are given in Table 2.

2. Stress-Corrosion Tests

Since testing of 1-inch thick plate in the short-transverse direction was the concern of this work, a specimen geometry as shown in Fig. 2 was designed. A set of 24 lever-arm loading stress-corrosion units was constructed for making the tests. Several of the units illustrating the manner of loading are shown in Fig. 3. In order to obtain more uniform distribution of load over the test specimen, two Ti-6Al-4V titanium alloy pins at right angles were placed between the specimen and the loading ram. A 0.192-inch diameter pin was placed in the groove in the top of the specimen, and a second pin having a radius of curvature of 0.10 inch in the longitudinal profile and 0.190 inch minimum diameter was placed at right angles to the first. Thin rubber sheet served to insulate the lower pin from the specimen, and the stainless steel loading ram was coated with Stop-Off strippable lacquer. Corrosion test media employed were the following basic solutions: (1) 57 g NaCl, 10 ml 30% H₂O₂, and water to make 1 liter, and (2) 3 g NaCl, 36 g CrO₃, 30 g K₂Cr₂O₇ and water to make 1 liter. Initially an addition of 0.01 g Aerosol wetting agent was made to the solutions. However, when it was discovered that this addition apparently had an adverse effect on the stabilities of the solutions, and that there was a significant difference in behavior of 7075, depending on whether or not the solution contained the Aerosol addition or not, the Aerosol was left out. The specimens were immersed continuously, and the solutions were changed daily except Saturdays and Sundays. The load was fully applied to the test specimen before the corrosion medium was added to the container.

3. Tensile Tests

Longitudinal tensile specimens of the geometry shown in Fig. 4 were tested in an Instron machine of 10,000-pound capacity. A crosshead speed of 0.1 in./min was employed. The tensile test specimens were taken from the edge of the plate.

4. Microprobe Analysis

Electron beam microprobe analysis was made of the second-phase particles present in standard commercial 7075-T6. The surface of examination was the plane parallel to the rolling plane and at the center of the plate. The unit employed was built by Cambridge Instruments Limited. The surface was prepared metallographically and etched to reveal the second-phase particles. The region for examination was then marked off by microhardness indentations, and after this the surface was repolished. (Past experience indicates that etching sometimes leaves surface films which obscure the analytical results.) The microhardness indentations made it easy to locate the region for examination. X-ray images were made of K_a emissions of aluminum, chromium, copper, magnesium, and zinc. Reflected electron images were also made.

5. Residual Stress Determination

Residual stresses were determined in the short-transverse and long-transverse directions on the plane perpendicular to the rolling direction at the approximate center of the plate thickness. The determination was made on a sample from each of the 7075-T6 materials of the investigation. The two-exposure method described in Barrett (5) was used. This method has the advantage that it obviates the need for an exposure of the material in the unstressed state. In order to get the residual stress in the two directions three exposures were required: one with the X-ray beam perpendicular to the specimen surface, a second with the surface rotated in the horizontal plane 45° toward the beam, and the third with the surface rotated in the vertical plane 45° toward the beam. A fine coating of annealed silver powder was sprinkled on the polished specimen face to act as a standard for specimen-to-film distance calibration. The (511) reflection for Cu K α radiation of both silver and aluminum were used for the distance and stress measurements, respectively. The camera was oscillated back and forth through 15° during the exposures in order to smooth out the spottness of the large-grained materials.

C. Results and Discussion

1. Microstructures

An indication of the relative as-cast grain sizes of the 7075 alloy prepared materials is given by Fig. 5, which shows macrostructures of the tops of the ingots which were cut off and discarded and sections of small test ingots which were poured with each heat. Some porosity is apparent in the high-purity, coarse grain size ingot. Microstructures of the planes parallel to the rolling plane at one-half plate thickness, perpendicular to the long transverse direction, and perpendicular to the short transverse direction for the four materials are shown in Figs. 6 through 13. For each material two groups of microstructures are presented: one showing the grain structure primarily, and the other showing the distribution of second-phase particles. It is immediately apparent that there is a marked difference in the grain structures of the various materials, and that these differences may be related to the differences in the distribution of second-phase particles. In the standard commercial material the second-phase particles tend to be distributed in layers parallel to the rolling plane; while in the remelted material the particles are much less directionally distributed. Casting practice, no doubt, had some influence in causing this difference; however, the amount of reduction in processing perhaps also contributed. The commercial material probably experienced a reduction ratio of about 10:1, while the laboratory prepared material experienced reduction ratios of about one-half this amount. Qualitatively, it is apparent that the remelted commercial material has a much finer grain size than the standard, and the grains are much less elongated.

The high-purity, coarse grain size material contained only occasional groups of second-phase particles, and elongation of grains was less marked than in the remelted commercial material. As shown in the photomicrographs in Fig. 13, the high-purity, fine grain size material contained virtually no

resolvable second-phase particles. It may be noted that the coarse grain size and fine grain size materials have approximately the same grain size after processing and final heat treatment. However, the grains in the former are elongated, and those in the latter are equiaxed. It is considered that the equiaxed grain structure of the fine grain size material is due primarily to two factors: the fine as-cast grain size, and the scarcity of second phase particles. The first factor contributes to the second in that second-phase particles in the as-cast state are smaller and more uniformly distributed and, as a consequence, are more readily taken into solution. The second factor means that there are few inhibitions to isotropic grain growth during the final solution heat treatment.

Comparison of the microstructures of the fine grain size materials shows that the commercial-purity material contains considerable quantity of second-phase particles, while the high-purity material contains virtually none. The results of the chemical analyses (Table 2) show that the high-purity laboratory prepared melts contain only 50% as much copper as the commercial material, both as-received and remelted. The disparity in the amount of second-phase particles between the two types is probably due to this composition difference.

2. Microprobe Analysis of Second-Phase Particles in 7075-T6

Second-phase particles in commercial 7075-T6 on the plane parallel to the rolling plane at one-half plate thickness were examined in the microprobe analyzer. The specific areas analyzed are shown in Fig. 14. The regions labeled I and II were scanned at a magnification of about 200X, and the smaller regions labeled A and B were scanned at a magnification of about 2000X.

In the photomicrograph, region I is observed to contain large quantities of gray particles and a patch of two-phase particles which are black and gray. The electron image of this region is shown in Fig. 13. (The microprobe images are mirror images of the photomicrograph in Fig. 14.) Relative to the matrix, intensity differences in the electron image derive from two sources: (1) differences in surface elevation which cause shadows or intensified reflection, for example, note the microhardness impressions in Fig. 18; and (2) differences in average atomic number of phases present. In the case of the latter, second phase particles having higher average atomic number than the matrix produce light areas (relative to the matrix) in the electron image; and particles which have lower average atomic number than the matrix produce dark areas in the electron image. The electron image indicates that the phase which appears to be black is actually depressed below the surface, suggesting that it was attacked during polishing operations.

The Mg K α image of region I is shown in Fig. 16 and indicates magnesium enrichment in the area where the two-phase particles are located. The Al K α image of this region showed the gray particles to be poor in aluminum. Images due to Zn K α and Cr K α indicated uniformity with respect to zinc and chromium. A Cu K α image of zone A in region I is

shown in Fig. 17. The gray particles are shown to be copper-rich and, in view of the other evidence, appear to be CuAl₂ (or Al₂CuMg).

The electron image of region II is shown in Fig. 18, and it too indicates that the darker two-phase particles across the center of the region are, at least in part, below the level of the matrix surface. Not all of the darker spots in Fig. 18 appear to be artifact caused by depressions in the surface. It appears that a few of them are indicative of the presence of a phase having lower average atomic number than the matrix. Again, the Al and Cu K α images show that the large gray particles are both aluminum-poor and copper-rich and they are, apparently, CuAl₂ (or Al₂CuMg). The Al K α image of zone B in region II is shown in Fig. 19, and shows that the darker, two-phase particles are aluminum-poor; also the Cu K α image showed them to be slightly copper-poor. The findings that these two-phase particles: (1) are poor in aluminum, (2) are poor in copper, (3) contain areas of enrichment of magnesium, and (4) are indicated to have lower average atomic number than the matrix suggest that at least one of the phases is a magnesium compound.

3. Tensile Test Results

Results of tensile tests of longitudinal specimens taken from the 7075 materials are summarized in Table 2. The tensile properties of the two commercial purity materials are in fair agreement. The strength properties, except fracture strength, of the two high-purity materials were in close agreement; and the yield strengths were about 20,000 psi below those of the commercial materials. The fractured specimens are shown in Fig. 20. One segment of each of the specimens is shown. Note particularly the character of the fracture of the high-purity, coarse grain size material. Much of the fracture surface of these specimens consists of parallel planes all being parallel to the rolling direction and, consequently, parallel to the stress axis of the test specimens. Much of surface area of these parallel planes was covered by a thin, dark film which can be discerned in Fig. 20. This film has not been identified as yet. The specimens of commercial material showed a tendency to fracture in a similar manner; however, the steps were much smaller and there was no sign of a film under magnifications up to 30X.

4. Residual Stress

Results of the residual stress determinations are summarized in Table 3. All of the measurements were hampered to some extent by the relatively large grain sizes of the materials. This problem was much greater for the high-purity materials than for the commercial materials. These results indicate that residual stress in the short-transverse direction was least favorable in the commercial material; in order of increasingly favorable residual stress in the short-transverse direction the materials are: commercial, grain refined; high-purity, fine grain size; and high-purity, coarse grain size.

5. Stress-Corrosion Test Results

The results of stress corrosion tests on the 7075-T6 materials are given in Tables 4, 5, and 6; Table 6 summarizes results for tests in NaCl-H₂O₂-Aerosol solution. These data, as shown in Fig. 21, indicate that the commercial material and the high-purity, fine grain size material behave similarly. Only specimens of commercial, grain-refined and high-purity, coarse grain size survived for more than 1000 hours. However, two specimens of the latter material failed immediately. (Specimens which failed immediately are plotted at 0.1 hour.) Since the load was first applied to the specimen and then the corrosion medium was added, such failures were not due solely to loading, and by all indications were truly the result of stress corrosion. A total of eleven specimens of the high-purity, coarse grain size material were tested in three solutions. Of these, five failed immediately. This was the only material to fail in times of less than 0.1 hour.

Results for tests in NaCl-H₂O₂ solution (without Aerosol) are given in Table 5, and plotted in Fig. 22. The commercial, grain-refined and the high-purity, coarse grain size materials behaved similarly to their behavior in the solution with the Aerosol addition. However, the commercial material performed more poorly, and the high-purity, fine grain size material performed better.

Results for tests in CrO₃ solutions are given in Table 6. Considering the commercial material, testing in CrO₃ solution containing Aerosol made up five months before resulted in an average life for two specimens of 0.35 hour, while testing in solution made fresh daily resulted in an increase in the average life of more than a hundredfold. Curiously, testing in CrO₃ solution containing no Aerosol and made fresh daily gave much the same result as testing in the old solution containing Aerosol. Data for the various materials in CrO₃ (no Aerosol) solution are plotted in Fig. 23. These results show that the materials have increasing resistance to stress-corrosion cracking in the order: commercial; commercial, grain refined; high-purity, coarse grain size; and high-purity, fine grain size. It is of interest to note that specimens of the high-purity coarse grain size material either fail immediately or perform better than the specimens of the other materials. This indicates the presence of a statistical factor in regard to the test section of these specimens.

Surface observations and microstructural examination were made of selected exposed stress-corrosion specimens. These observations are summarized in Table 7. The salient fact to come out of this examination pertains to grain structure. The microstructural observations were made on the plane perpendicular to the long-transverse direction. Grain structures were: layered as depicted in Fig. 6b, irregular as in Fig. 10c, or equiaxed as in Fig. 12b. With few exceptions, specimens which failed in less than 100 hours had the layered type microstructure; and specimens which survived for more than 100 hours, including those which did not fail in 1000 or more hours, had irregular or equiaxed grain structures. Of particular interest is the high-purity, coarse grain size material, specimens of which either failed in less than 0.1 hour or were quite resistant to failure. All specimens of this material which failed immediately had the layered type

grain structure, and the failure-resistant specimens had irregular grain structures. A similar generalization applied for the commercial, grain refined material--that is, two of the four specimens exhibiting short lives in CrO₃ solution were examined and found to have layered grain structure; while four specimens which did not fail in 1000 hours in NaCl-H₂O₂-Aerosol and NaCl-H₂O₂ solutions were found to have irregular grain structures. The generalization with respect to this material must be tempered by the fact that both layered and irregular grain specimens were in no case tested in the same environment as far as is known. However, not all specimens were examined metallographically. In the case of the high-purity coarse grain size material a second factor seems to have been involved that may explain why specimens of this material were the only ones to fail in less than 0.1 hour. This was the occasional presence of patches involving a few grains of a microconstituent which caused rather severe attack of the grain boundaries under the action of the etchant. (Keller's was used for both the light etching to reveal the distribution of microconstituents and the heavy etching to develop the grain structure.) In Table 7 this is referred to as "black grain boundary network." Apparently the most susceptible type of microstructure combined the layered grain structure with the microconstituent responsible for the black grain boundary network.

The variations in the final structure of a given material was, no doubt, related to the variation in the as-cast structure of the ingot and the somewhat different thermal and working history of the various parts of the ingot.

D. Summary and Conclusions

It was hypothesized that the poor resistance to stress-corrosion cracking in the short-transverse direction of wrought, high-strength aluminum alloys was due to the layered grain structure characteristic of these materials. Insoluble phases and phases resulting from nonequilibrium conditions during solidification tend to accumulate in the grain boundaries of the as-cast structure. In subsequent working the grains are flattened out into plates. During the rather severe solution heat treatment applied to these age-hardenable alloys, grain growth tends to proceed until it is inhibited by the barrier of second-phase particles which encased the original as-cast grains. This results in planes of weakness or of high susceptibility to stress-corrosion cracking parallel to the direction of working. Stressing in the short-transverse direction results in crack propagation along such planes. The primary objective of this study was to determine whether altering the as-cast microstructure--through changes in the melting and casting practice--would affect the final wrought and heat treated microstructure and whether this, in turn, would influence stress-corrosion behavior.

Four 7075-T6 materials in the form of 1-inch plate were investigated: (1) commercial; (2) commercial, remelted to refine grain size; (3) high-purity, coarse grain size; and (4) high-purity, fine grain size. The following determinations and tests were made: residual stress in the plane perpendicular to the rolling direction and in the short and long transverse directions; tensile tests of longitudinal specimens, and stress-corrosion tests in the short-transverse direction. Comparisons were made of the

microstructures of the various materials. Also, microprobe analysis was used to determine the major microconstituents present in the commercial material.

The commercial material had the characteristic layered grain structure; the commercial, grain-refined and the high-purity, coarse grain size materials exhibited a variation in grain structure from layered to irregular; and the high-purity, fine grain size material was equiaxed. Of special interest from the results of the tensile tests was the fact that the fracture surfaces of the high-purity, coarse grain size material contained a considerable area of parallel planes in the longitudinal direction. Much of the surface of these planes appeared to be covered by a black film.

Stress-corrosion media for most of the testing were: NaCl-H₂O₂ solution and NaCl-CrO₃-K₂Cr₂O₇ solution. In the former solution the commercial material was the least resistant to stress corrosion; the high-purity, coarse grain size material was next; and the commercial, grain refined and high-purity, fine grain size materials were the most resistant. In the latter solution the materials in order of increasing resistance to stress corrosion were: (1) commercial; (2) commercial, grain refined; (3) high-purity, coarse grain size; and (4) high-purity, fine grain size. The high-purity, coarse grain size material was unique in that specimens either failed immediately or they survived for 500 or more hours. Microstructural examination of the exposed specimens showed that specimens which failed immediately had the layered grain structure similar to that of commercial material, and specimens which had long life had irregular grain structure. The commercial, grain refined material behaved similarly in that short-lived specimens had the layered grain structure, whereas long-lived specimens had irregular grain structure. This observation with respect to the commercial, grain refined material must be tempered by the fact that, as chance would have it, the layered grain structure (short lived) specimens were tested in CrO₃ solution while the irregular grain structure (long lived) specimens were tested in NaCl-H₂O₂ solutions. Another characteristic of the high-purity, coarse grain size material was the presence of a grain boundary constituent in patches involving a few grains which etched very rapidly giving the appearance of a black grain boundary network. One might readily associate this with the black film observed on the tensile test fracture surfaces of the high-purity, coarse grain size material; however, this relationship has yet to be established.

Residual stresses in the short transverse direction were indicated to be least favorable for the standard commercial plate, and most favorable for the high-purity, coarse grain size material, the highest value being about +3000 psi. It does not appear that residual stress played a significant role in these stress-corrosion tests.

The results give general support to the hypothesis upon which this study was based. For the 7075 aluminum alloy, stress-corrosion susceptibility is related to microstructure, and one important factor in the control of the final microstructure of wrought material is the distribution of second-phase particles in the as-cast state.

II. PART II - STRESS CORROSION OF SST CANDIDATE MATERIALS

A. Introduction

Under certain conditions of laboratory testing, titanium alloys have exhibited susceptibility to stress corrosion at elevated temperatures when in the presence of chloride salts (6, 7). The temperature range in which stress-corrosion cracking has been observed is from about 550° to about 900°F. Much of the structure of the trisonic transport will operate in this temperature range. Therefore, a study was undertaken to determine the kinetics of sea salt stress-corrosion cracking of three representative candidate materials for structural applications in the trisonic transport. Materials selected for study were Ti-8Al-1Mo-1V, in the annealed condition; AM 350, 20 per cent cold rolled and PH 15-7Mo RH 1050.

B. Experimental Methods

Sources of the materials were as follows: The Ti-8Al-1Mo-1V in the form of 0.018 and 0.062 inch thick sheet materials and the AM 350 in the form of 0.025 inch thick sheet were supplied by Mr. William F. Brown, Jr., Chief, Strength of Materials Branch, Lewis Research Center, NASA. The chemistry of these materials is given in Table VIII. The PH 15-7Mo was purchased locally. The chemistry of the PH 15-7Mo was unavailable; however, it was certified aircraft quality.

Test specimens were of the geometry shown in Fig. 24. All specimens were transverse, since specimens of this orientation appear to be less resistant to factors which cause failure than longitudinal specimens. For testing in the presence of a notch a 1/16 in. hole was made in the center of the specimens. Such configurations represented theoretical stress concentrations, K_t , of 2.8 and 2.9 for the 3/8 and 1 in. width specimens, respectively. For stress-corrosion testing this hole was filled with a paste obtained by concentrating sea water by evaporation. In order to prevent the salt from getting on the face of the specimen, the area surrounding the hole on either side was coated with Boothguard "S" (Guard Coating Corp.) strippable lacquer. The specimen was placed on a hot plate and the salt plate was put into the hole. After evaporation of the salt paste to dryness the lacquer coating was readily stripped off.

Preliminary to beginning the kinetics study, specimens of the selected materials were tensile tested and surveyed for stress-corrosion behavior. Tensile tests were conducted on an Instron 10,000-lb capacity machine at a crosshead speed of 0.1 in/min. Stress-corrosion exposures were made in lever arm (20:1 ratio) loading type creep testing units.

Crack growth propagation was indicated by measuring resistance over a gage length by means of a precision Kelvin bridge. The test apparatus is shown schematically in Fig. 25. For the Ti-8Al-1Mo-1V alloy, potential leads across the gage section were 0.018 x 1/8 in. strips of the same material spot-welded to the specimen with approximately 1/8 in. between the

edges of the strips. Titanium wire (A-55), 0.050 in. diameter, was spot-welded to these strips to complete the resistance-measuring leads. A thermocouple was spot-welded to the specimen just below the gage section. With the exception of the final experiment the current leads were clamped to the pull arms. For the final experiment the current leads were spot welded to the specimen as indicated in Fig. 25. The change was made because the former arrangement resulted in a variable error in the resistance measurement due to variation in the resistance between the lower power lead clamp and the contact points of the resistance measuring leads.

In order to determine the relation between crack length and change in resistance, center hole specimens of 3/8 in. width of Ti-8Al-1Mo-1V were used. A one mil wide notch on one side of the hole was cut by abrading with one mil diameter tungsten wire coated with a paste consisting of alumina and Johnson's cutting wax thinned with automotive transmission oil. The notches were cut approximately 8 mils deep. Crack extension was obtained by tension-tension fatigue loading. The data obtained are given in Fig. 26. Each of the vertical bars represents a single specimen. After running the crack, the specimens were heated to 1000°F for 1 hour in air, to discolor the crack face. The specimens were then pulled to fracture and the average crack length determined. The data represented by circles were determined on a single specimen which remained in the machine under load while the crack length was measured by means of microscopic observation on the surface. The accuracy of the last two points is very questionable since the crack was propagating very rapidly. The point represented by the triangle is the average change in resistance of nine specimens before and after cutting the 8-mil deep notch by means of tungsten wire-alumina abrasion.

It was found that the measured resistance was very sensitive to bending and torsional loads on the specimens. Apparently, this was due to changes in contact resistances in the circuit. The scatter in the data in Fig. 26 is believed to be due, for the most part, to the fact that the contact resistances were not the same before and after the fatigue cracks were put in.

C. Results and Discussion

Results of tensile tests of the materials for evaluation are given in Table 9. The thinner gage (0.018 in.) Ti-8Al-1Mo-1V alloy material exhibited yield point behavior. To the author's knowledge this is the first time yield point phenomena have been observed in a commercial titanium alloy, although such behavior has been reported for experimental alloys of titanium with nitrogen. Stress-strain curves for the 0.0625 in. material exhibited simply a flattening of the curve after initial yielding. This observation of yield point phenomenon is perhaps due to the fact that these specimens were tested at a strain rate of 0.07 in/in/min, while the usual rate for titanium alloys is 0.003 to 0.005 in/in/min.

The AM 350 CR material exhibited a rather low yield strength, because it was not tempered after the cold reduction. This was the result of a misunderstanding. (It was assumed that this material was supplied in the condition for evaluation--that is, cold reduced and tempered 825°F-3hr.)

The first two specimens of PH 15-7Mo tested had tensile elongations of only about one-half specification value, and the 90° (relative to stress axis) fractures suggested some surface damage or defects. A second pair of specimens were surface ground to remove 1.5 mils from each side. Grinding was done in the transverse direction because of the difficulty of holding this thin material on the magnetic bed for longitudinal grinding. Ductility improved slightly, and necking occurred. However, the fractures were again at 90°. Four additional specimens were surface ground, in the longitudinal direction. These showed no further improvement in properties over the specimens that had been ground in the transverse direction.

Results of the preliminary survey of stress-corrosion behavior under conditions in which sea salt is packed into a notch consisting of a 1/16 in. diameter hole in the center of the specimen are summarized in Table 10. Stress-corrosion cracks were found in the Ti-8Al-1Mo-1V specimens. However, it does not appear that AM 350 CR and PH 15-7Mo RH 1050 are susceptible to stress-corrosion under the conditions of investigation. These materials are not recommended for service above 700°F, and it appears that exposure to a temperature of 800°F, per se, causes deterioration of mechanical properties due to metallurgical instability. Two unnotched specimens of PH 15-7Mo alloy were coated with sea salt to determine if accelerated oxidation caused by the salt would lead to premature failure or cracking. Both specimens were exposed for 1000 hours under a stress of 75,000 psi. Temperatures were 700°F for one specimen and 800°F for the other. Tensile properties after the exposures were as follows:

Spec. No.	Temp., °F	YS, ksi	UTS, ksi	Elong., %
P-15(3/8)	700	238	246	4.4
P-16(3/8)	800	246	254	2.8

Ripplin (9) likewise found no indication that AM 350 was susceptible to sea salt stress corrosion at 650°F.

The first attempts to obtain kinetics data on the Ti-8Al-1Mo-1V alloy were made employing 0.018 in. thick material. A 3/8 in. wide gage section was used. The specimens were exposed at 650° or 800°F under stresses of 40,000 or 55,000 psi. Cracks developed in the specimen; however, changes in the resistance due to reduction in the cross-sectional area were masked by changes in the contact resistances between the current leads and the resistance-measuring leads during the course of the exposures. The sensitivity of the precision Kelvin bridge is 0.04 per cent. Therefore, as the base-line resistance is reduced, the absolute change in resistance that can be measured is reduced and consequently the size of the crack that can be detected. In the last attempt 0.062 in. sheet specimen with a 1 in. wide gage section was used. This specimen represented an increase in cross-sectional area over the prior specimens of about 10 times, thus having a lower gage resistance by the same magnitude. In order to minimize errors due to changes in contact resistances the current leads were spot-welded to the test specimen about 1/2 in. outside the resistance-measuring leads. The current leads consisted of 0.018 by 1/8 in. strips of Ti-8Al-1Mo-1V alloy which were spot-welded to the specimen. Copper wire of 18 gage was spot-welded to these

strips. This specimen was unloaded at the end of each day, but temperature was maintained. The specimen was at temperature approximately 24 hours before the load was applied. Resistance began to change within 1/2 hour after loading. For the first 23 hours resistance increase was fairly regular, there being a 4-hour and a 2-hour period in which resistance was constant. At this point the change in resistance indicated a net reduction in cross-sectional area of 1.6 per cent. From this time to 60 hours the resistance values changed rather erratically, being much higher than values projected from the data up to 23 hours. However, after 60 hours, the resistance values returned to the curve projected from the initial values. The final resistance values indicated a reduction in cross-sectional area of 5 per cent.

When the specimen was taken out, it was found that contrary to previous experience the salt had crept outside the hole. Also, spots of salt, apparently the result of spattering during the exposure, were found on the surface. Apparently the salt became molten during the exposure as has been observed and reported (8). The spattering may have been caused by gas generated during the exposure. Five cracks were observed, extending from the center hole and varying in length from 0.020 to 0.050 in. Also cracks were observed under the salt spots caused by spattering.

This technique of monitoring resistance to measure crack growth kinetics is considerably more difficult when applied at elevated temperatures than for room-temperature studies. As yet, the erratic resistance changes have not been resolved. However, the technique appears to be promising.

REFERENCES

1. F. A. Crossley and L. F. Mondolfo, "Mechanism of Grain Refinement in Aluminum Alloys," Trans. AIME, 191 (1951), pp. 1143-8.
2. F. A. Crossley, R. D. Fisher, and A. G. Metcalfe, "Viscous Shear as an Agent for Grain Refinement in Cast Metal," Trans. AIME, 221 (1951), pp. 419-20.
3. F. A. Crossley, "Magnetic Stirring; A New Way to Refine Metal Structures," Iron Age, 186 (10), (September 8, 1960), pp. 102-4.
4. Metals Handbook, Vol. 1, 8th Ed., American Society for Metals, Novelty, O. (1961), pp. 936, 948, 1118.
5. C. S. Barrett, Structure of Metals, McGraw-Hill Book Co., Inc., New York (1943), pp. 273-5.
6. "The Salt Corrosion of Titanium Alloys at Elevated Temperature and Stress," TML Report No. 88, Defense Metals Information Center (PB i21637).
7. F. A. Crossley, C. J. Reichel, and C. R. Simcoe, "The Determination of the Effects of Elevated Temperatures on the Stress Corrosion Behavior of Structural Materials," WADD TR 60-191, Armour Research Foundation under Contr. No. AF 33(616)-6392, (May 1960).
8. R. I. Jaffee, F. C. Holden, and H. R. Ogden, "Mechanical Properties of Alpha Titanium as Affected by Structure and Composition," Trans. AIME, 200 (1954), pp. 1282-90. F. A. Crossley, Discussion to above paper, Trans. AIME, 203 (1955), pp. 717-8.
9. E. J. Rippling, "Elevated Temperature Stress Corrosion of High Strength Sheet Materials in the Presence of Stress Concentrators," Quarterly Progress Reports under Contract NASr-50 (1961-62).

TABLE I
MATERIALS FOR 7075 ALUMINUM ALLOY MELTS

Materials	Purity, %	Supplier	Form	Impurities, wt%
Aluminum	99.99 min.	Aluminum Co. of America	1 lb ingot	0.002Cu 0.003Fe 0.001Si 0.001Mg
Chromium	99.43	Elchrome	Lump	0.045C 0.033O
Copper	99.9	Fisher Scientific Co.		
Magnesium	99.8 min.	Dow Chemical Co.	1 lb sticks	Maximum: 0.02Cu 0.01Pb 0.15Mn 0.001Ni 0.01Sn 0.05 ea. others

TABLE 2
CHEMISTRY OF 7075 MATERIALS

Element	Comml. Nominal Composition*	Analytical Results					
		As-received		Commercial 7075		Remelted Comm. No. 1 No. 2	
		Sample No. 1	Sample No. 2	7075	7075 Grain	7075 Grain	7075 Grain
Chromium	0.18-0.40	0.19	----	0.19	0.01	0.14	0.28
Copper	1.2-2.0	1.71	1.58	1.62	0.88	0.76	1.28
Iron	0.7	0.27	0.29	----	----	----	0.00
Magnesium	2.1-2.9	2.52	2.56	2.53	1.91	1.87	2.13
Manganese	.3	0.04	----	0.04	----	0.01	0.28
Silicon	0.5	0.16	0.10	----	0.07	----	0.00
Titanium	0.2	0.04	----	0.02	0.03	0.01	0.36
Zinc	5.1-6.1	4.77	4.74	3.95	4.76	4.45	5.47

* Compositions are in weight per cent.

TABLE 3
TENSILE TEST PROPERTIES OF 7075-T6 MATERIALS

Material	Designation	Yield Strength (0.2% offset), ksi	Ultimate Tensile Strength, ksi	Fracture Strength, ksi	Elong. (in 1 in.), %	Reduction in Area, %
Commercial standard	A	83.8 85.0 <u>84.4</u>	92.8 94.2 <u>93.5</u>	103.3 104.6 <u>104.0</u>	10.5 10.2 <u>10.4</u>	10.4 10.7 <u>10.6</u>
Commercial purity, grain refined	1.	77.5 79.7 <u>78.6</u>	85.9 87.6 <u>86.8</u>	94.1 98.3 <u>96.2</u>	9.1 9.3 <u>9.2</u>	8.6 11.0 <u>9.3</u>
High-purity, coarse grain size	11	61.3 60.1 <u>60.7</u>	67.1 65.8 <u>66.4</u>	76.5 70.4 <u>73.4</u>	10.6 8.7 <u>9.6</u>	14.5 6.4 <u>10.4</u>
High-purity, fine grain size	10	61.2 59.0 <u>60.1</u>	67.2 65.6 <u>66.4</u>	89.5 83.2 <u>86.4</u>	13.6 16.2 <u>17.4</u>	40.7 36.2 <u>39.4</u>
	Avg.					

TABLE 4
RESIDUAL STRESS OF 7075-T6 MATERIALS

Material	Residual Stress, psi	
	Short Transverse Direction	Long Transverse Direction
Commercial	+2940	+8820
Commercial, grain refined	+1470	+1470
High-purity, coarse grain size	-2940 to -4370	-2940 to -4370
High-purity, fine grain size	-1470	-1470

Note: The error produced in stress measurement by a ± 0.1 mm error in reading the films of the commercial purity materials is approximately ± 1500 psi. The coarse grain size of the high-purity materials made accurate ring measurement considerably more difficult; and the error for these may be ± 3000 to ± 4500 psi.

TABLE 5
STRESS-CORROSION RESULTS FOR 7075-T6 MATERIALS
IN NaCl-H₂O₂-AEROSOL SOLUTION

Material	Specimen No.	ksi	Stress		Time to Failure, hr
			% Yield Strength		
Commercial	A-12	48.4	57.1		433.1
	A-13	44.3	52.3		445.7
	A-14	65.4	77.1		59.0
	A-15	60.3	71.1		65.3
Commercial grain refined	12-1	40.0	50.9		1006.8NF*
	12-2	39.8	50.7		1006.8NF
	12-3	55.4	70.5		1009.4NF
	12-4	55.9	71.1		167.7
High-purity coarse grained	11-4	39.1	64.3		1006.8NF
	11-7	36.2	59.5		Immediate
	11-5	41.7	69.0		Immediate
	11-6	38.0	62.9		1009.5NF
High-purity fine grained	10-1	38.4	63.9		369.3
	10-2	38.2	63.5		387.7
	10-3	37.2	61.8		319.6
	10-4	40.1	66.6		< 750

* NF--no failure, stopped at time given.

TABLE 6
STRESS-CORROSION RESULTS FOR 7075-T6 MATERIALS
IN NaCl-H₂O₂ SOLUTION

Material	Specimen No.	ksi	Stress	Time to Failure, hr
			% Yield Strength	
Commercial	A-26	42.4	50	97.1
	A-27	42.4	50	123.7
	A-22	63.6	75	63.8
	A-23	63.6	75	36.7
Commercial grain refined	12-5	58.9	75	1343.9NF*
	12-6	58.9	75	< 270
High-purity coarse grained	11-15	30.4	50	1032.1NF
	11-17	30.4	50	Immediate
	11-8	45.6	75	Immediate
	11-9	45.6	75	1343.9NF
High-purity fine grained	10-5	45.2	75	1056.6
	10-6	45.2	75	613.8

* NF -- no failure, stopped at time given.

TABLE 7
STRESS-CORROSION RESULTS FOR 7075-T6 MATERIALS
IN CHROMATE SOLUTIONS

Materials	Specimen No.	Stress		Time to Failure, hr	Comments
		ksi	% Yield Strength		
Commercial	A-16	43.9	51.8	0.3	Old solution containing Aerosol
	A-17	44.6	52.6	0.4	
	A-18	31.5	37.1	98.4	Fresh solution containing Aerosol
	A-19	45.9	54.1	23.6	
	A-22	42.4	50	0.3	Fresh solution without Aerosol
	A-35	42.4	50	0.4	
	A-24	63.6	75	0.2	
	A-25	63.6	75	0.4	
	12-11	39.3	50	2.8	Fresh solution without Aerosol
	12-12	39.3	50	3.9	
Commercial grain refined	12-7	58.9	75	0.6	
	12-8	58.9	75	2.1	
	11-18	30.4	50	1032. INF*	Fresh solution without Aerosol
	11-10	45.6	75	512.0	
High-purity coarse grained	11-12	45.6	75		
	10-11	30.1	50	534.4	
	10-12	30.1	50	530.3	
	10-7	45.2	75	46.8	
High-purity fine grained	10-8	45.2	75	90.6	

* NF -- no failure, stopped at time given.

TABLE 9

SUMMARY OF SURFACE AND METALLOGRAPHIC OBSERVATIONS
ON EXPOSED STRESS-CORROSION SPECIMENS OF 7075-T6 MATERIALS

Solution	Specimen No.	Exposure Conditions	Observations on Plane Perpendicular to Long-Transverse Direction				
			Stress, ksi	Time, hr	Observations on Surface	General Comments	Microstructural Grain Structure
$\text{NaCl-H}_2\text{O}_2$ - <i>Aerosol</i>	A-12	48.4	433	Obscured	Pits	Layered	
	A-14	65.4	59	Cracks not evident	Pits	Layered	
	12-1	40.0	NF*	---	---	Irregular	
	12-2	39.8	NF	---	---	Approaching layered, grains not very long	
	12-3	55.4	NF	---	---	Irregular	
	11-4	39.1	NF	Relatively few second-phase particles	Black gb network.	Irregular. Black gb network.	
11-6	38.0	NF	---	---	---	Same as 11-4	
	11-7	36.2	< 0.1	---	---	Layered. Black gb network.	
10-1	38.4	369	---	Fracture not at min. cross section	Equiaxed. Appears to be mechanical fracture.		
$\text{NaCl-H}_2\text{O}_2$	A-22	63.6	37	Large cracks above fracture.	Pits	Layered	
	12-5	58.9	NF	Pits at CuAl_2 aggregates	---	Irregular	
	11-8	45.6	< 0.1	Fracture not at min. cross section	---	Layered. Black gb network.	
	11-9	45.6	NF	Pits	---	Equiaxed. Black gb network	
	10-6	45.2	614	Several cracks below fracture	---	Equiaxed	

TABLE 8 (cont.)

Solution	Specimen No. [†]	Exposure Conditions			Observations on Surface	Observations on Plane Perpendicular to Long-Transverse Direction	
		Stress, ksi	Time, hr	Microstructure [‡]		General Comments	Grain Structure
CrO_3 -Aerosol	A-18	31.5	98	Cracks not evident Large cracks	Pits on compression side ---	Same as A-25 Minor pits, hair-line cracks	Layered Layered
	A-19	45.9	24				
CrO_3	A-24	63.6	0.2	Multiple cracks Few cracks	---	Large crack containing band of matrix	Layered Layered
	A-25	63.6	0.4				
CrO_3 -Aerosol (old solution)	A-28	42.4	0.3			Same as A-25 Minor pits, hair-line cracks	Layered Layered
	12-7	58.9	0.6				
CrO_3 -Aerosol (old solution)	12-8	58.9	2.1			Layered Layered. Black g's network.	Black g's network.
	11-10	45.6	<0.1				
CrO_3 -Aerosol (old solution)	11-12	45.6	512			Irregular Equiaxed superimposed on layered substructure	Irregular Equiaxed superimposed on layered substructure
	10-7	45.2	47	Single crack above fracture	---		
CrO_3 -Aerosol (old solution)	A-16	43.9	0.3			Fine cracks Large crack containing band of matrix	Layered Layered
	A-17	44.6	0.4				

[†] A - commercial; 12 - commercial, grain refined; 11 - high-purity, coarse grain size; and 10 - high-purity, fine grain size.

[‡] NF - no failure in 1000 or more hours.

g's - grain boundary.

TABLE 9

CHEMISTRY OF TRISONIC TRANSPORT
CANDIDATE MATERIALS

Alloy	Heat No.	Chemical Analysis
Ti-8Al-1Mo-1V (0.018 in.)	V-1551	7.8 Al, 1.1 Mo, 1.1 V, 0.09 Fe, 0.032 C, 0.003-0.009 H, 0.013 N.
Ti-8Al-1Mo-1V (0.062 in.)	V-1554	7.8 Al, 1.1 Mo, 1.1 V, 0.08 Fe, 0.021 C, 0.004 H, 0.013 N.
AM 350 23% CR	W-23227-1	16.50 Cr, 4.29 Ni, 1.63 Mn, 0.21 Si, 0.10 N, 0.084 C, 0.009 P, 0.007 S, balance Fe.

TABLE 10
TENSILE TEST PROPERTIES
OF SST CANDIDATE MATERIALS

Alloy	Condition	Thickness, in.	Yield Strength, (0.2% offset) ksi	Ultimate Tensile Strength, ksi	Elong., %	Comments
Ti-8Al-1Mo-1V	Annealed	0.018	136	139	18.0	Yield point phenomenon observed for both speci- mens.
		137	139	139	18.5	
AM 350	CR (20% cold reduced)	0.024	116	234	16.4	25-26° fracture (to horizontal).
	RH 10 ^{5.5}	0.025	116	237	16.4	
F71 15-7Mo		203	214	2.6	90° fracture, low elongation.	
		208	214	3.0		
0.022		216	224	3.6	Surface ground in trans- verse direction to remove 1.5 mils from each side. Necks at 45° angle; how- ever, fractures at 90°.	
		223	230	3.5		
0.022		211	218	3.3	Surface ground longitudi- nally to remove 1.5 mils from each side. Necks at 30° angle, fractures at 90°.	
		211	216	3.9		
0.026		218	223	3.7	Surface ground longitudi- nally to remove 2.5 mils from each side. Necks at 30° and 38° angles, fractures at 90°.	
		218	224	3.6		

TABLE II
STRESS-CORROSION SUSCEPTIBILITY SURVEY
OF SST CANDIDATE MATERIALS
Notched ($K_t = 2.8$ or 2.9) Specimens

Material*	Spec. No.	Exposure Conditions			Post-Exposure Tensile Properties			Comments
		Temp., °F	Stress, ksi	Time, hr	YS, ksi	UTS, ksi	Elong., %	
Ti-3Al-1Mo-1V (3/8)	T2-20	None	---	---	143.5	146.5	0.3	scc + 0.01 in. scc's from face as well as from edge of hole. scc 0.02 in.
	T2-2	650	25	50	----	88.0	0.0	
	T2-8	650	63	200	----	121.0	0.0	
T2-7	800	25	100	----	77.4	0.0	----	----
Ti-8Al-1Mo-1V (1)	T2-11	650	63	50	----	129.8	---	Failed in pin hole, no evidence of scc.
	T2-14	650	25	100	----	132.0	---	
T2-18	650	63	50	----	120.6	---	----	----
AM 350 CR (3/8)	A-18	None	---	---	135.5	210.5	5.1	Necked, rust-colored discoloration.
	A-8	650	100	50	172.5	202.0	2.1	
A-9	650	100	100	100	168.0	207.0	6.0	Necked.
A-10	800	40	1003	1003	----	----	----	No evidence of scc.
A-12	800	40	1002	1002	----	----	----	No evidence of scc.
A-14	800	75	1005	1005	147.0	230.0	6.9	No evidence of scc.
A-17	800	75	1000	1000	146.0	210.0	14	----
AM 350 CRT (1)	A-13	650	100	200	----	202.0	----	----
	A-1	800	40	200	----	----	----	
PH 15-7Mo (3/8)	P-11	None	----	----	219.5	219.5	0.33	No yielding.
	P-12	None	----	----	219.5	219.5	0.32	
	P-7	800	40	1000	254.5	0.0	0.0	
P-8	800	40	1000	195.5	0.0	0.0	0.0	No yielding.
P-9	800	75	1000	----	----	----	----	----
P-10	800	75	217.4	----	253.0	0.0	0.0	Failed during exposure.
P-14	700	75	1000	----	----	----	----	----

* Thickness as follows: Ti-8Al-1Mo-1V, 0.01"; AM 350 CRT, 0.024; and PH 15-7Mo, 0.022 in.; numbers in parentheses give width of gage section in inches.

+ SCC = stress-corrosion crack.

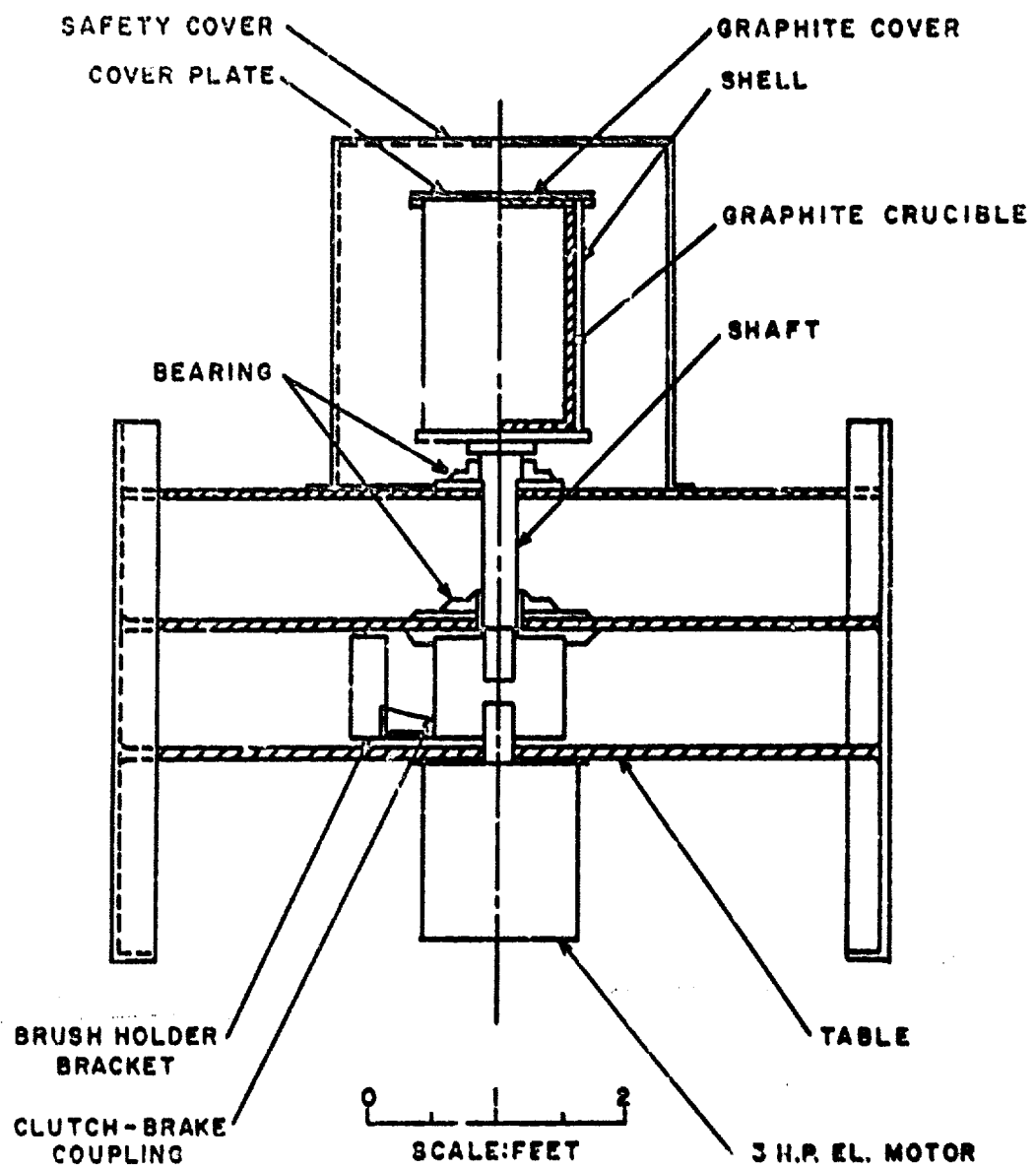


FIG. 1 - SHEAR INDUCER

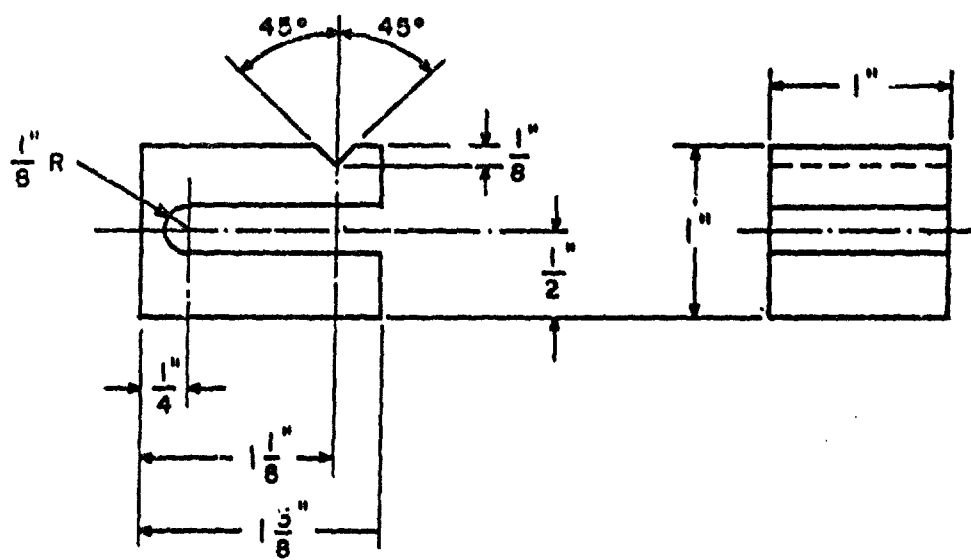


FIG. 2 - STRESS CORROSION TEST SPECIMEN FOR EVALUATION OF SUSCEPTIBILITY IN THE SHORT-TRANSVERSE DIRECTION OF PLATE.



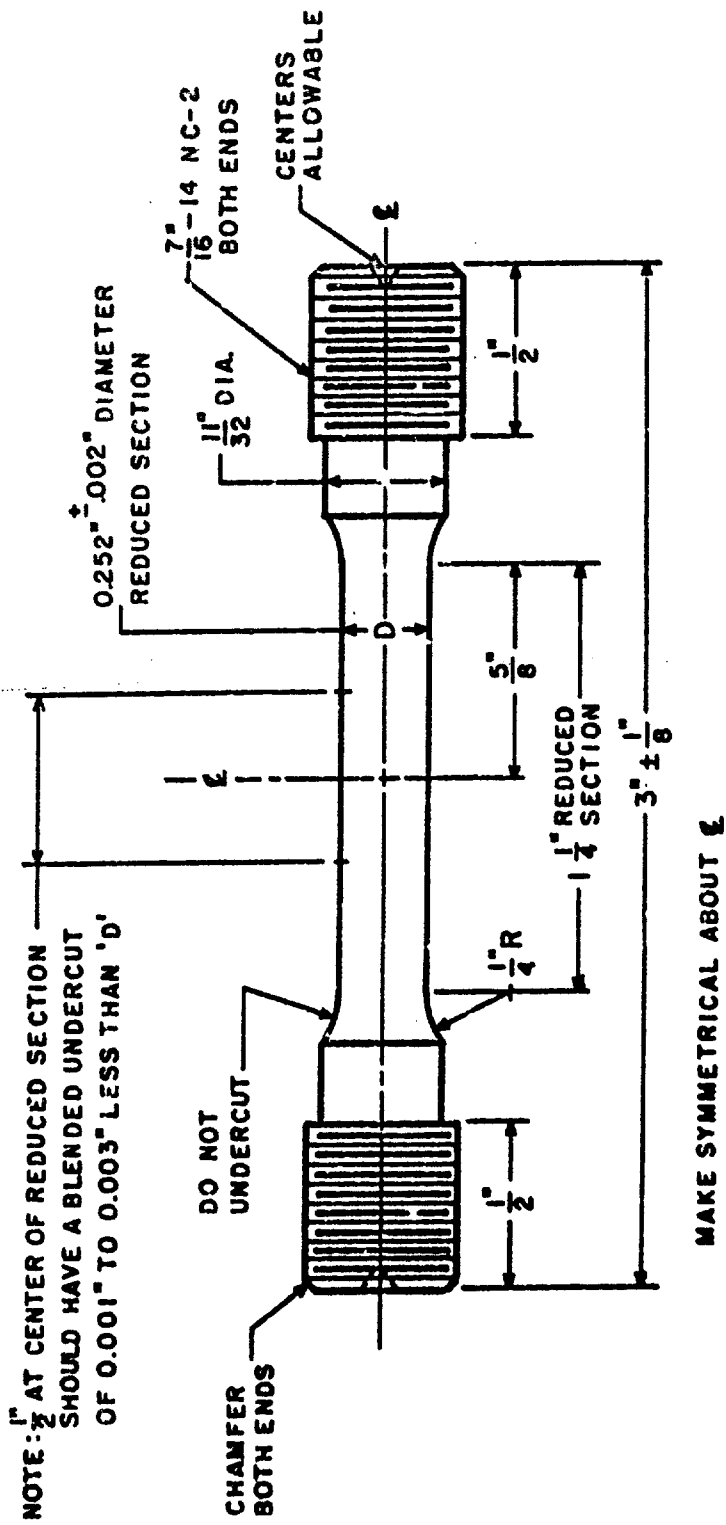


FIG. 4 - TENSILE TEST SPECIMEN FOR 7075-T6 MATERIALS.

X4/5

Fig. 5 - Macrographs of castings of 7675 alloy: Left—high purity, fine grain size; Center—high purity, coarse grain size; and Right—remelted commercial stock, fine grain size.





N 23246

X100

(a) Plane parallel to the rolling plane.



N 23248

X100

(b) Plane perpendicular to the long
transverse direction.



N 23247

X100

(c) Plane perpendicular to the roll-
ing direction.

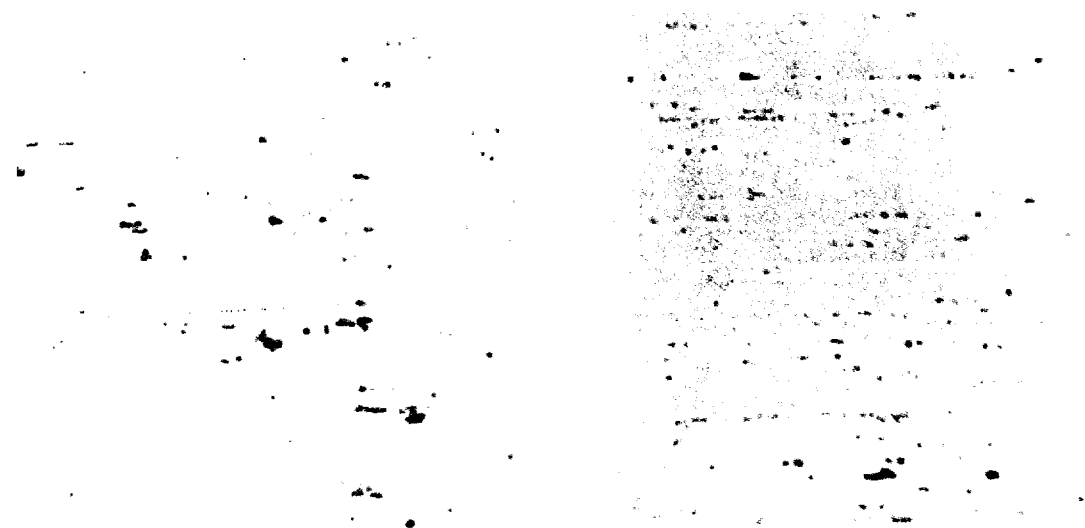
Fig. 6 - Microstructures of 7075-T6 commercial plate 1-inch thick Etchant:
Keller's.



N 23245

X250

(a) Plane parallel to rolling plane.



N 23243

X250

(b) Plane perpendicular to the long
transverse direction.

N 23244

X250

(c) Plane perpendicular to the roll-
ing direction.

Fig. 7 - Microstructures showing distribution of second-phase particles in 7075-T6 commercial plate 1-inch thick. Etchant: 1% conc. HF in water.



N 23970

X100

(a) Plane parallel to the rolling plane.



N 23971

X100

(b) Plane perpendicular to the long
transverse direction.



N 23972

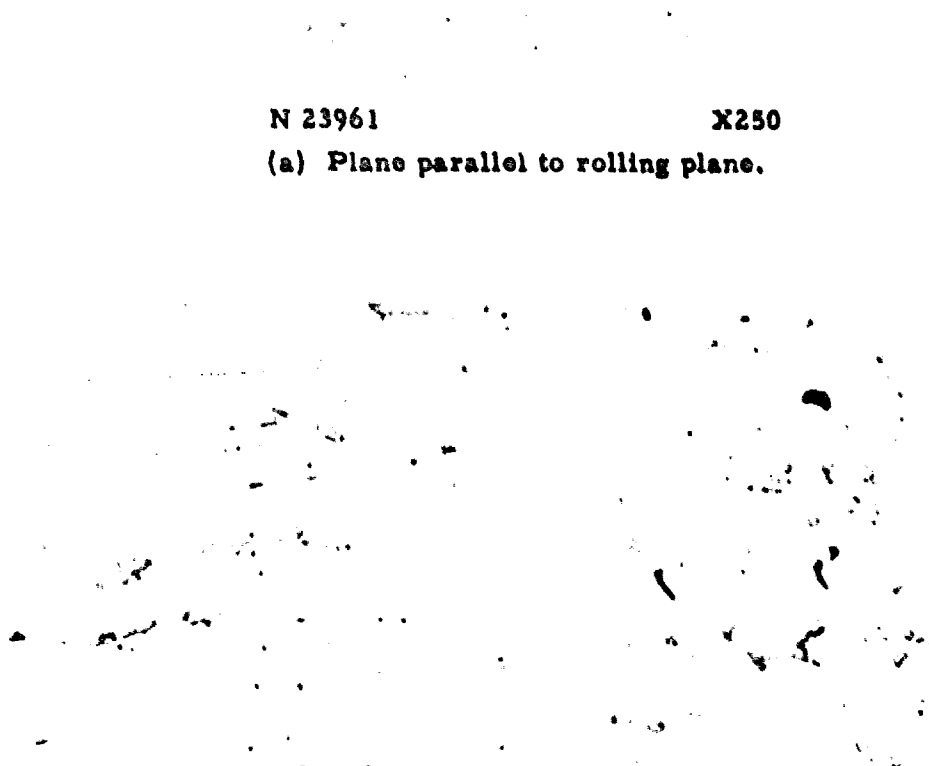
X100

(c) Plane perpendicular to the roll-
ing direction.

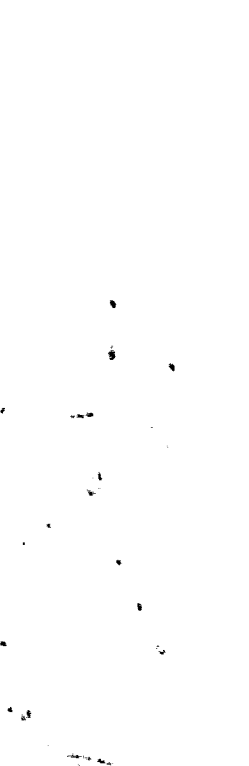
Fig. 8 - Microstructures of 7075-T6 commercial purity plate 1-inch thick,
remelted and grain refined. Etchant: Keller's.



N 23961 X250
(a) Plane parallel to rolling plane.



N 23962 X250
(b) Plane perpendicular to the long
transverse direction.



N 23963 X250
(c) Plane perpendicular to the roll-
ing direction.

Fig. 9 - Microstructures showing distribution of second-phase particles in 7075-T6 commercial purity plate 1-inch thick, grain refined. Etchant: 1% conc. HF in water.



N 23967

X100

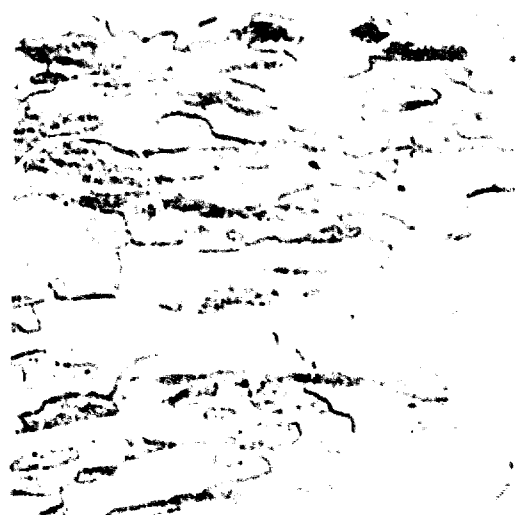
(a) Plane parallel to the rolling plane.



N 23968

X100

(b) Plane perpendicular to the long transverse direction.

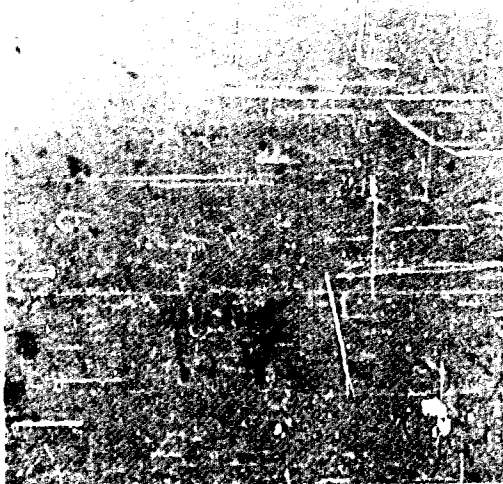


N 23969

X100

(c) Plane perpendicular to the rolling direction.

Fig. 10 - Microstructures of 7075-T6 high-purity plate 1-inch thick, coarse grain size. Etchant: Keller's.



N 23958

X250

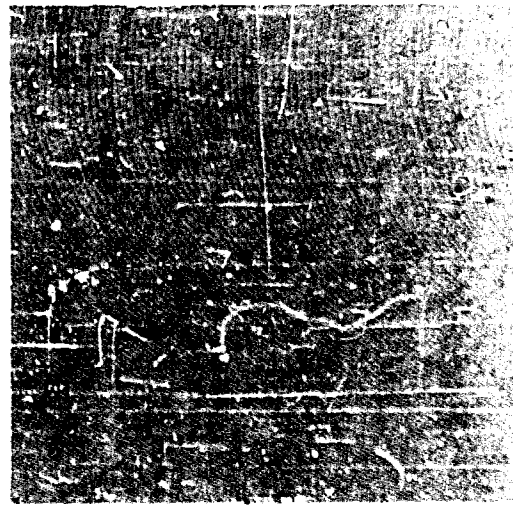
(a) Plane parallel to the rolling plane.



N 23959

X250

(b) Plane perpendicular to the long transverse direction.



N 23960

X250

(c) Plane perpendicular to the rolling direction.

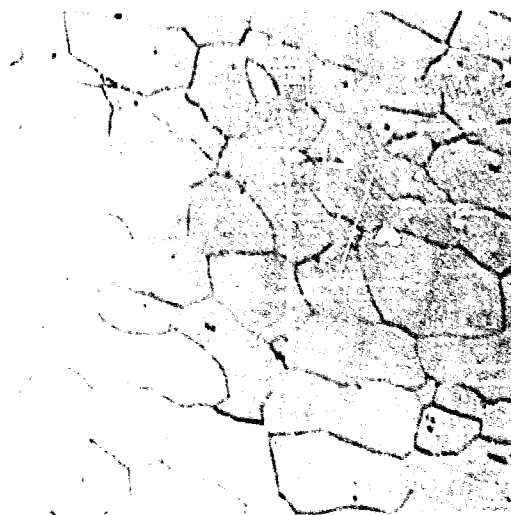
Fig. 11 - Microstructures showing distribution of second-phase particles in 7075-T6 high-purity plate 1-inch thick, coarse grain size. Etchant: 1% conc. HF in water.



N 23964

X100

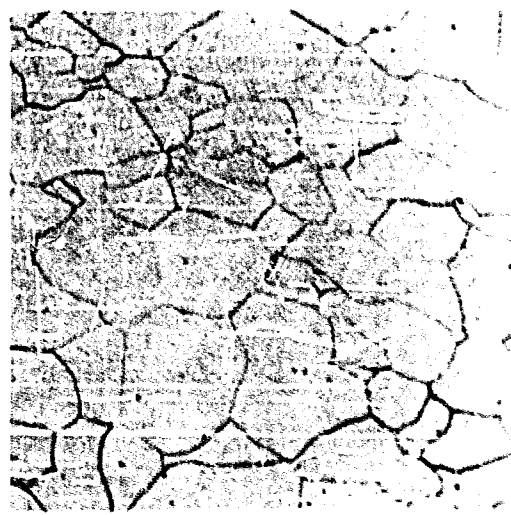
(a) Plane parallel to the rolling plane.



N 23965

X100

(b) Plane perpendicular to the long
transverse direction.



N 23966

X100

(c) Plane perpendicular to the roll-
ing direction.

Fig. 12 - Microstructures of 7075-T6 high-purity plate 1-inch thick, fine grain size. Etchant: Keller's.



N 23955

X250

(a) Plane parallel to rolling plane.



N 23956

X250

(b) Plane perpendicular to the long
transverse direction.

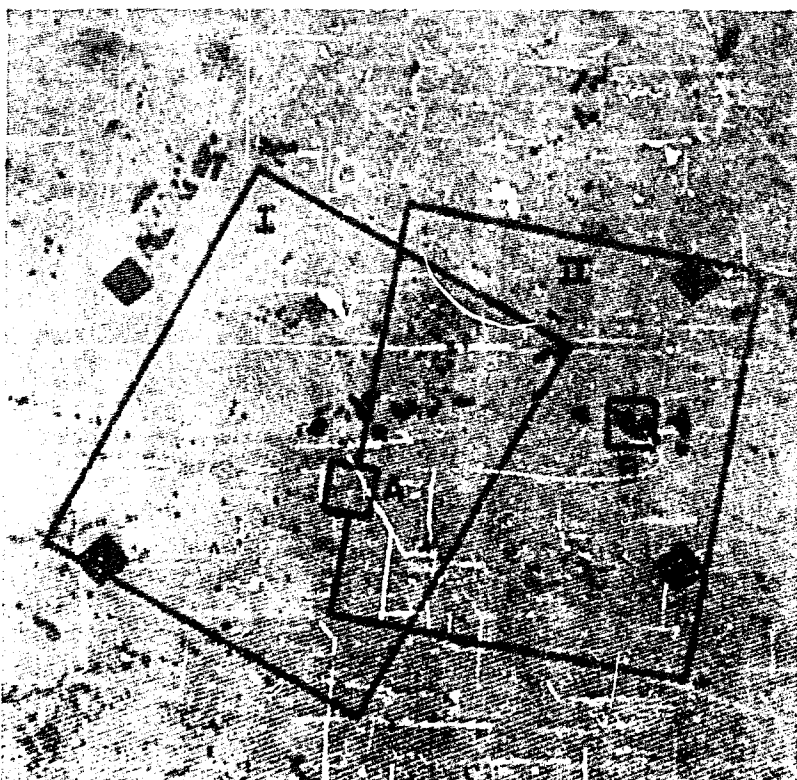


N 23957

X250

(c) Plane perpendicular to the roll-
ing direction.

Fig. 13 - Microstructures showing distribution of second-phase particles
7075-T6 high-purity plate 1-inch thick, fine grain size. Etchant:
1% conc. HF in water.



N 23774

X250

Fig. 14 - Areas on plane parallel to the rolling plane examined with the microprobe analyzer. Commercial 7075-T6 plate 1-inch thick. Unnotched. The gray particles are tentatively identified as CuAl_2 .



MP 345

X250

Fig. 15

Electron image of region I. Bright areas represent higher average atomic number than that of the matrix.



MP 349

X250

Fig. 16

Mg K α image of region I shows dark particles to be rich in magnesium.



MP 361

X1350

Fig. 17

Cu K α image of zone A of region I shows gray particles to be copper-rich.



MP 351

X250

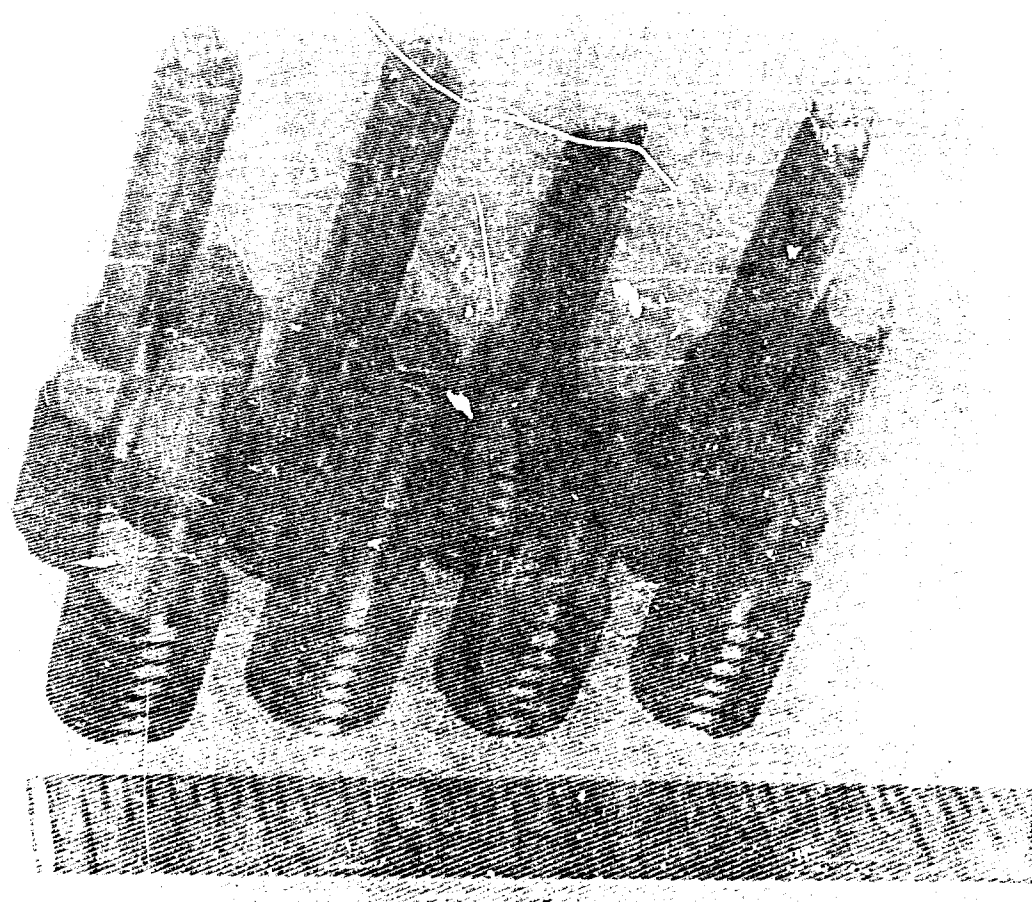
Fig. 18
Electron image of region II.



MP 364

X1350

Fig. 19
Al K α image of zone B in region II shows dark particles to be aluminum-poor.



H 26159

22

Fig. 20 - One end of each of the fractured tensile test specimens of 7075-T6 materials. From left to right: (1) commercial; (2) commercial, grain refined; (3) high-purity, coarse grain size; and (4) high-purity, fine grain size.

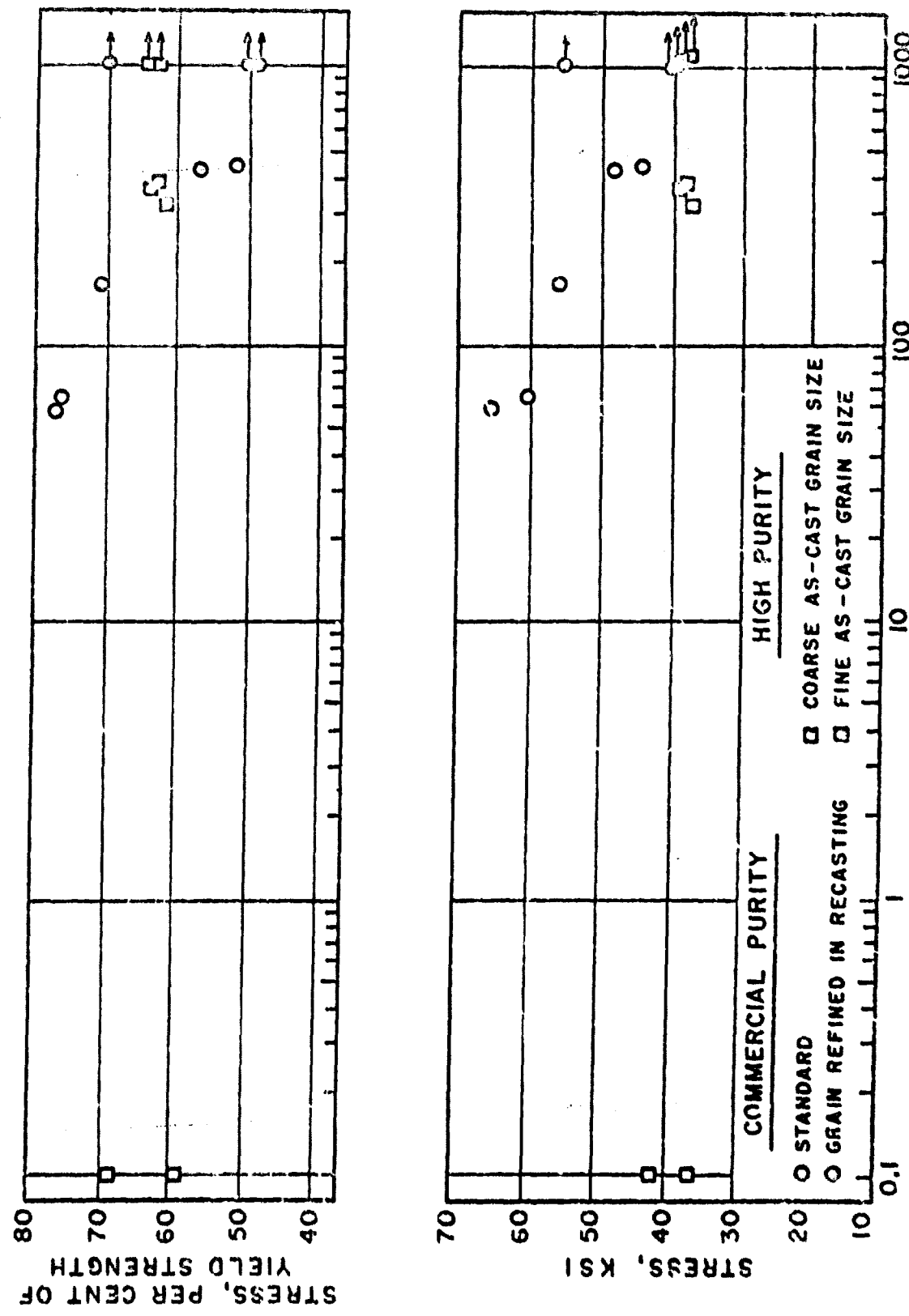


FIG. 21 - STRESS CORROSION RESULTS FOR 7075-T6 MATERIALS IMMERSSED IN DAILY CHANGED
BATH OF $\text{NaCl}-\text{H}_2\text{O}_2$ -AEROSOL SOLUTION.

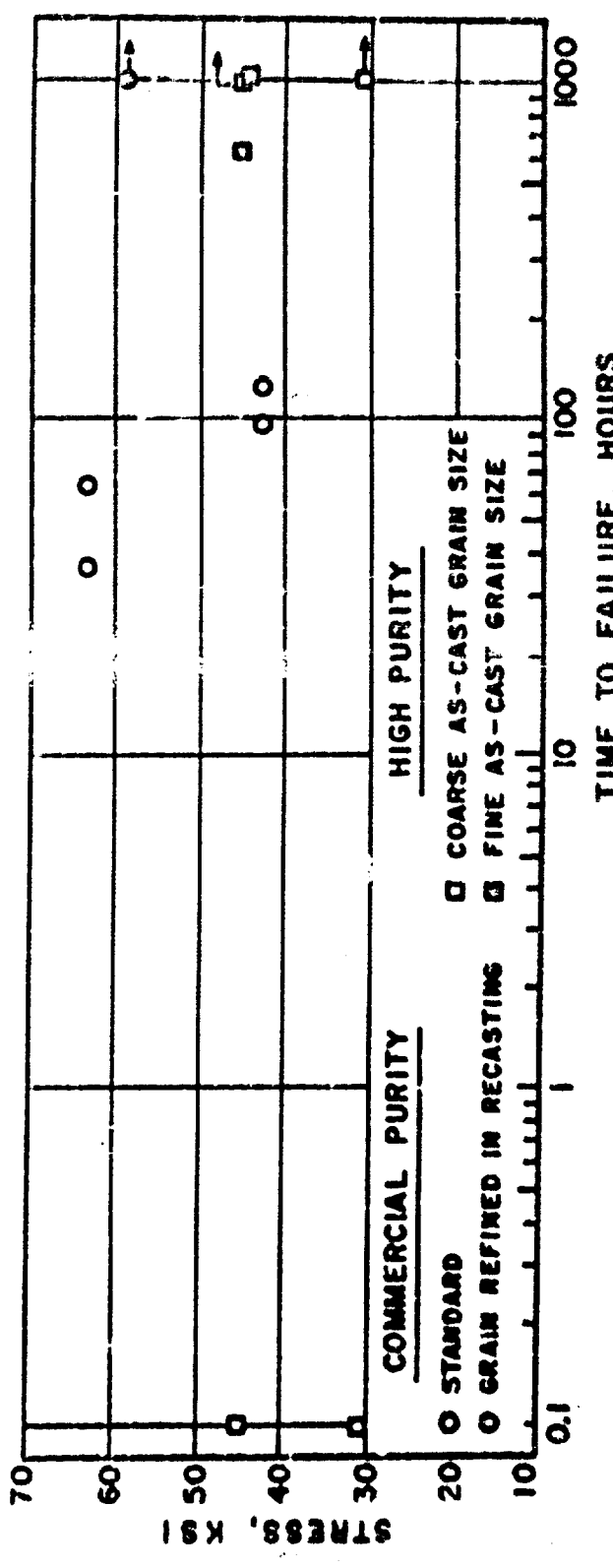
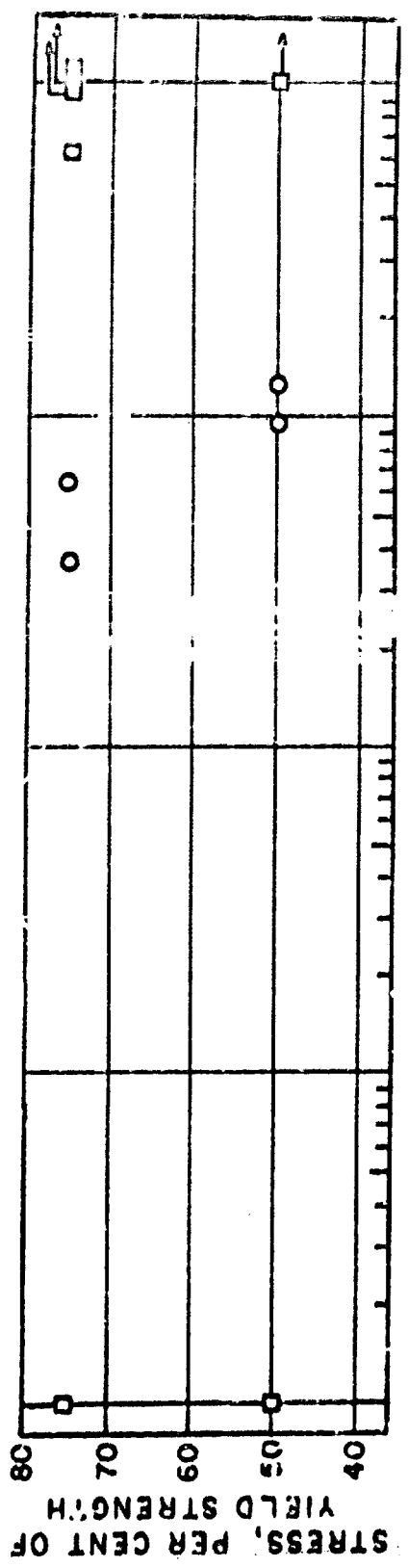


FIG. 22 - STRESS CORROSION RESULTS FOR 7075-T6 MATERIALS DIPPED IN DAILY CHANGED BATH OF $\text{NaCl} \cdot \text{H}_2\text{O}_2$ SOLUTION.

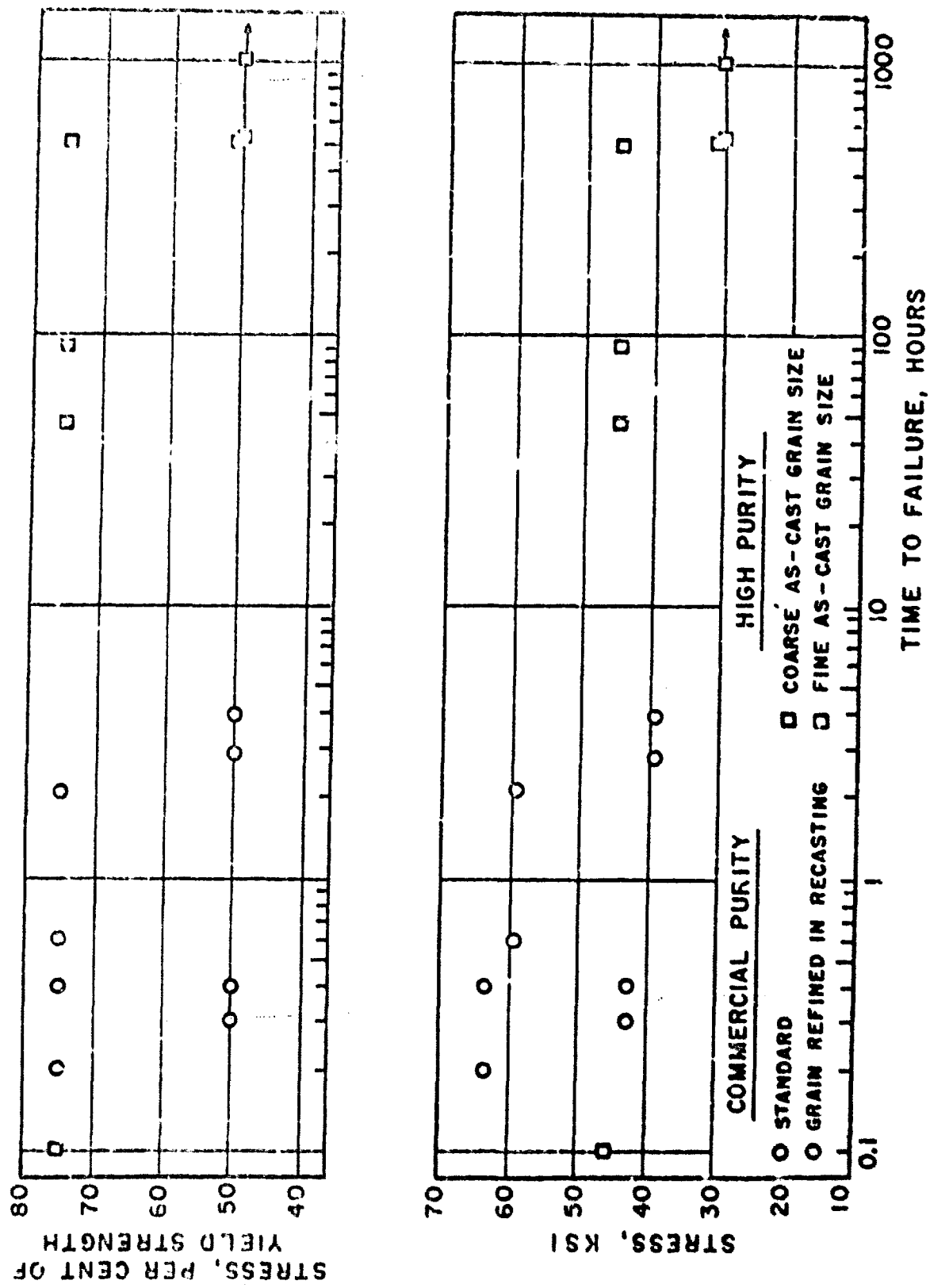
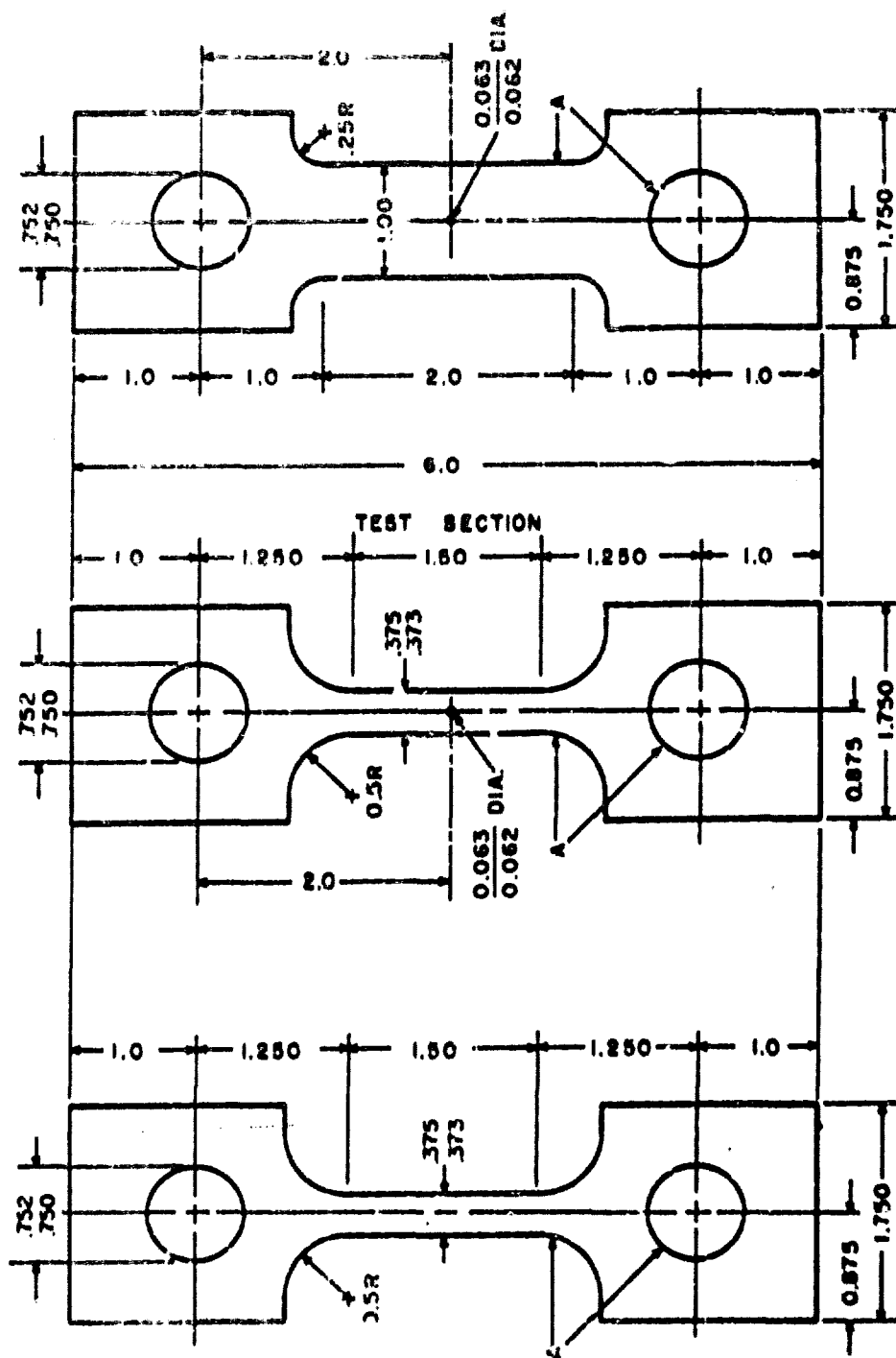


FIG. 23 - STRESS CORROSION RESULTS FOR 7075-T6 MATERIALS IMMERSSED IN DAILY CHANGED BATH OF CrO_3 SOLUTION.

FIG. 24 - SMOOTH (LEFT) AND NOTCHED (CENTER AND RIGHT) SHEET TENSION TEST SPECIMENTS.



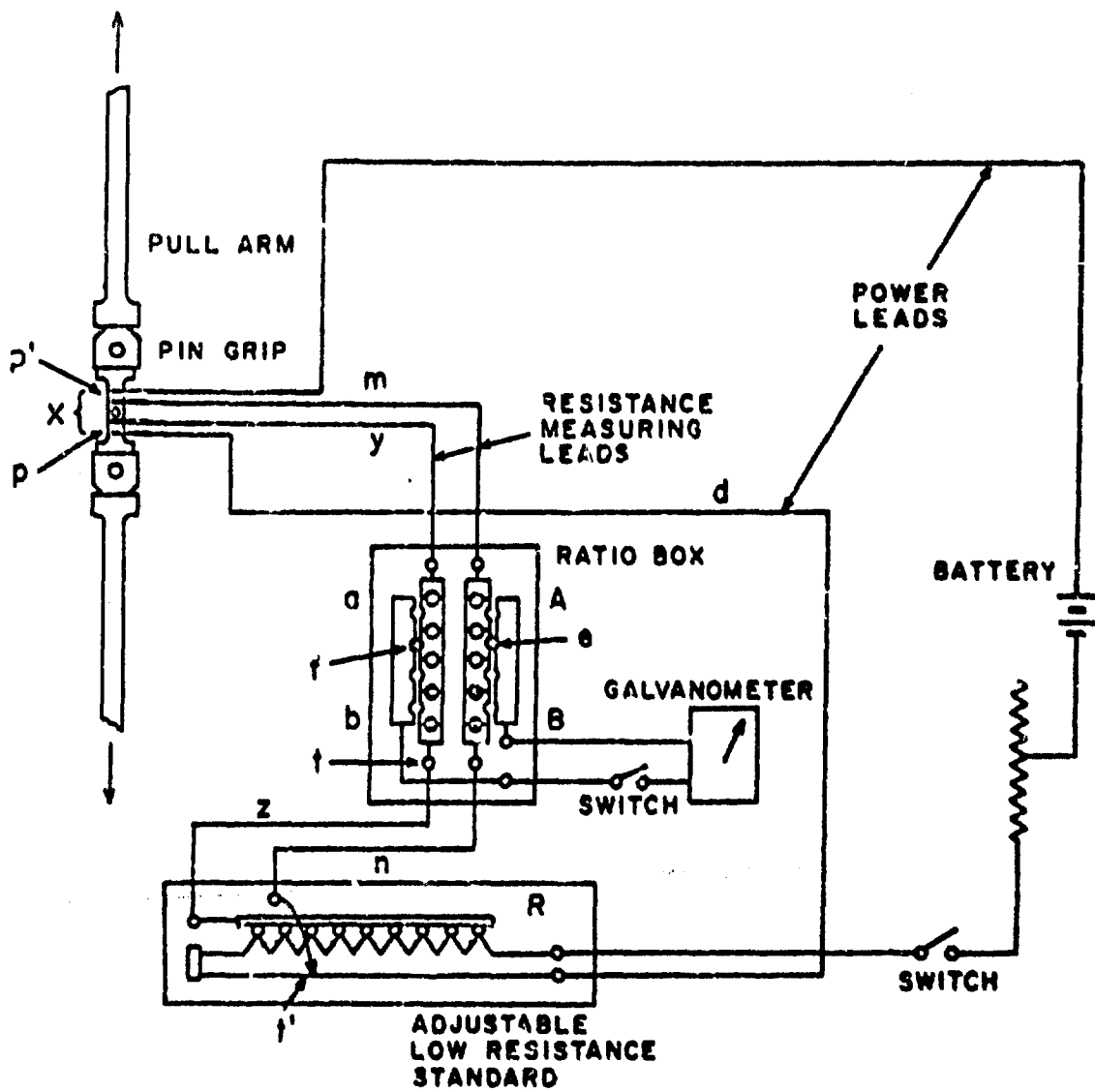


FIG. 25 - SCHEMATIC DIAGRAM OF APPARATUS FOR PRECISION MEASUREMENT OF RESISTANCE.

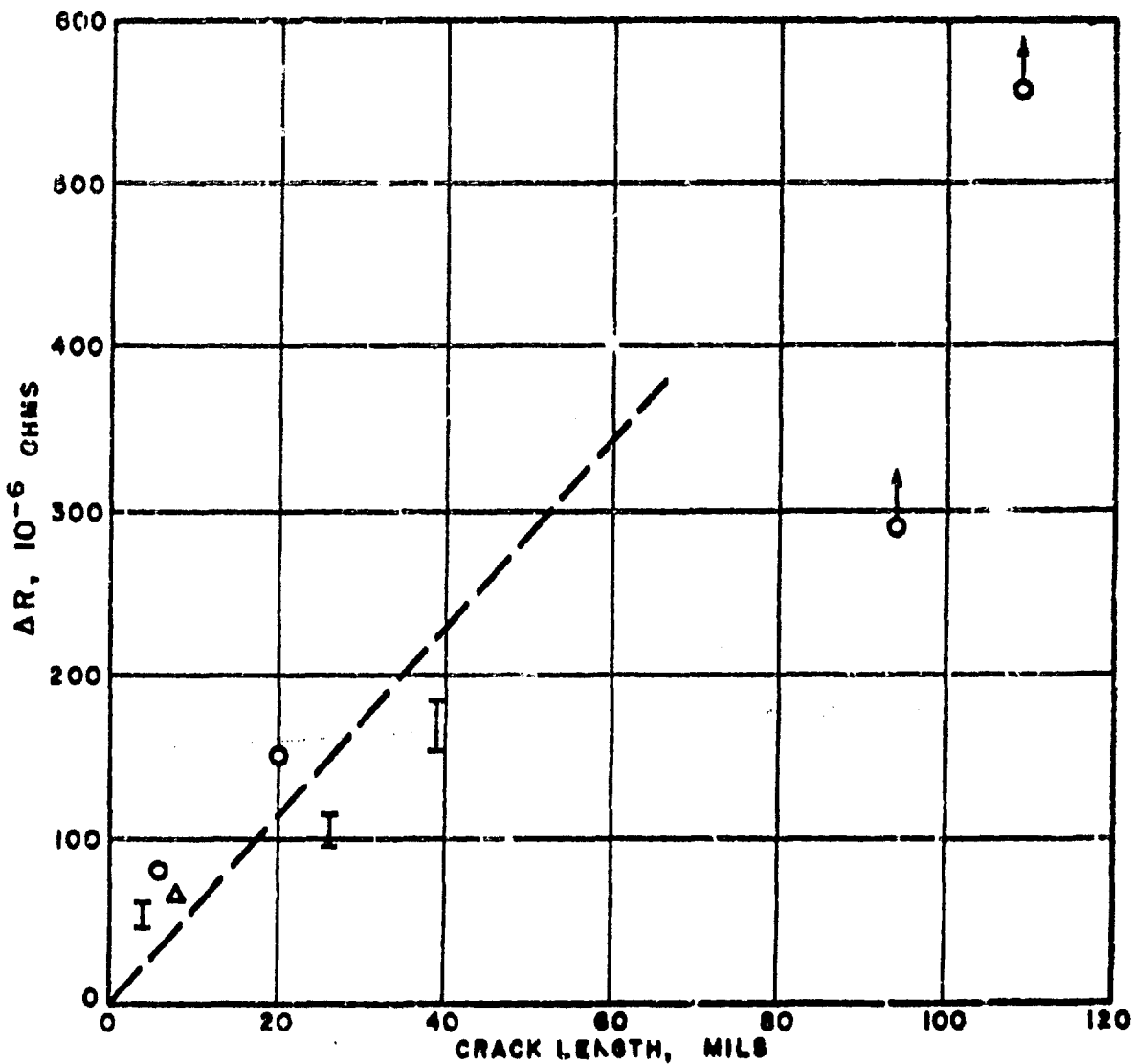


FIG. 26 - CHANGE IN RESISTANCE WITH CRACK LENGTH FOR Ti-8Al-1V SPECIMENS.

Aerospace Systems Division, Dir/31 Mater-
ials & Processes, Metals & Ceramics
Lab., Wright-Patterson AFB, Ohio.
DAB-TR-41-713, Pt. II RE-
SEARCH ON THE BASIC NATURE OF
STRESS CORROSION FOR VARIOUS STEELS
AT TOTAL ALLOYS AT 200 AND ELEVAT-
ED TEMPERATURE. Final report, Feb 63.
49p. locl num. - tables, 9 refs.

Declassified Report

Program objectives were to study effect of
interstructure on susceptibility to stress-
corrosion cracking in the short-transverse
direction of 1015-76 laminations alloy; and
to study the kinetics of stress-corrosion
cracking at high temp. of carbide suscep-
tible steels structures; applications in the tri-

concrete containing 2% in the presence of 20% salt. It was hypothesized that the poor resistance to chloride-corrosion of 7875-T6 was due to a layered type microstructure.¹ Short life was also claimed, with layered type of grain structures, and long life with irregular or equiaxed grain structures. The experimental results gave good support to the hypothesis.

PROBLEMS 37 trials for determining stress-
correlation function, by means of precision
measurement of resistance shear porosities.

1. Admixture Additives
2. Coatings of Amines
3. Deicer Technology (Molecular)
4. Heat Resistance
5. Salt Stress Cracking
- L. AFSC Proj 7135 Task 735106
- H. Concrete No. AF 33(614)-76
- III. Arrestor Runway Foundation Chicago, Ill.

~~UNCLASSIFIED~~ IV. Grossety, Fra
A. ARF-B236-12
V. Aral is ONS
VI. ASTIA collec
tions

Aeronautical Systems Directorate, Wright-Patterson Air Force Base, Ohio, has issued a report entitled "Program Objectives were: to study effect of microstructure on susceptibility to stress-corrosion cracking in the short-transverse direction of 7075-T6 aluminum alloy; and to study the kinetics of stress-corrosion cracking at high temp. of candidate materials for structural stiffeners in the tri-

ionic transport in the presence of sea salt. It was hypothesized that the pore resistance to cation-carrying of TOT-T6 was due to a layered type microstructure. Short life was associated with layered type of grain structure, and long life with intercalated grain structure. The experimental results gave lived support to the

Preliminary trials for determining species-specific resistance to insecticides by means of precision measurement of resistance when necessary.

CLASSIFIED

1. Administrative Affairs
2. Construction of All
3. Geography (Mechanical)
4. Near East
5. Sales Stress Control
6. AFSC Proj 7151
7. AFSC Proj 7151S
8. Contract No.
9. AF 3367-91-7611
10. Armenian Research Foundation
11. Chicago, IL

UNCLASSIFIED

IV. Crassley, Pres.
A. V. JEP-848-11
W. And Is OTS
T. ACTA case
class

卷之三